J. Physiol. (1981), **314**, *pp.* 595–633
With 23 text-figures
Printed in Great Britain

MEMBRANE CHARGE MOVED AT CONTRACTION THRESHOLDS IN SKELETAL MUSCLE FIBRES

BY P. HOROWICZ AND M. F. SCHNEIDER

From the Department of Physiology, University of Rochester School of Medicine and Dentistry, Rochester, New York 14642, U.S.A.

(*Received 26 February 1980*)

SUMMARY

1. The current I_Q due to membrane charge movement and the threshold pulse duration t_{th} required to produce microscopically just-detectable contraction were determined for pulses to a variety of membrane potentials in tendon-terminated short segments of cut frog skeletal muscle fibres voltage-clamped using a single gap technique.

2. The time course $Q(t)$ of membrane charge movement was calculated as the running integral of I_Q. The threshold charge Q_{th} moved by pulses which produced just-detectable contraction was estimated as $Q(t_{th})$.

3. Q_{th} was constant for pulses to potentials ranging from about -45 mV, the rheobase potential for contraction, to about -15 mV, where t_{th} was about 9 msec. The mean Q_{th} from fourteen fibres was 11·5 nC/μF, when the holding potential was about -100 mV.

4. Prepulses of 50 msec which were themselves sub-rheobase for producing contraction decreased the t_{th} for an immediately following test pulse. The total threshold charge moved during the prepulse and during t_{th} of the test pulse was equal to Q_{th} for the test pulse without prepulse.

5. Items 3 and 4 above indicate that t_{th} is determined by the time required to move a set amount of intramembrane charge, independent of the kinetics of the charge movement.

6. Steady partial fibre depolarization to between -70 and -55 mV increased t_{th} at all membrane potentials and elevated the rheobase potential for contraction. Slight further steady depolarization totally eliminated contraction.

7. Steady partial depolarization decreased the total ON charge movement Q_{ON} by about the same factor for pulses to all potentials tested.

8. Q_{th} for partially depolarized but still-contracting fibres remained approximately independent of membrane potential from rheobase to about 0 mV but was slightly less than Q_{th} for the same fibres when fully polarized.

9. Steady partial depolarizations which reduced the mean ($\pm$S.D.) ON charge movement Q_{ON} to 60 ± 8 % of its value under full polarization reduced Q_{th} to 86 ± 11 % of its full polarization value ($n = 10$). These steady partial depolarizations produced no change in the linear capacitance measured with hyperpolarizing pulses.

10. Contraction was completely abolished by steady partial depolarizations which reduced Q_{ON} to 41 % of its value under full polarization (mean of three runs). The

0022-3751/81/4840-0818 $07.50

maximum value of Q_{ON} was then 77 % of the Q_{th} value for the same fibres under full polarization.

11. A prolonged tail, a shoulder, a second rising phase or an early relatively high flat segment were successively evident in the I_Q records as the depolarizing pulse was successively increased to and beyond the rheobase potential for contraction. It was found that t_{th} either coincided with or occurred slightly later than the start of such tails, shoulders or second rising phases.

12. When test pulse I_Q records with and without immediately preceding sub-rheobase prepulses were shifted in time so that their t_{th} times coincided, the record with prepulse coincided with the later part of I_Q without prepulse. This indicates that sub-rheobase prepulses moved the initial portion of the I_Q that occurs during the test pulse alone, whereas they did not alter the latter portion of the test pulse I_Q.

13. A model was developed which accounts for charge movement's voltage dependence and kinetics and for the relationship between charge movement and just-detectable contraction in both the fully polarized and partially depolarized states.

14. The model proposes that Q be composed of two components. Component A is due to the voltage and time-dependent movement of charges between two sites located within the membrane and separated by a single energy barrier. Component B is instantaneously proportional to an integer power n of the fraction of component A charges which have crossed the barrier.

15. The I_Q time courses were best approximated using $n = 3$, with which both the relatively early and late portions of the experimental I_Q time courses could be reproduced. The best theoretical records obtained with $n = 3$ still passed below the shoulders, second rising phases and later parts of the early constant phases in the various experimental I_Q records. Theoretical records did fit accurately the I_Q time courses observed under steady partial fibre depolarization. The relatively small current not reproduced by the model may be an electrical accompaniment of the activation of calcium release or the elevation of internal free calcium levels in the space between the transverse tubules (T-tubules) and the sarcoplasmic reticulum.

INTRODUCTION

The preceding paper presented evidence that the single gap voltage-clamp technique can be used to monitor reliably membrane charge movement for pulses well beyond contraction thresholds of mechanically fully active muscle fibres (Horowicz & Schneider, 1981). The single gap technique thus provides an opportunity to investigate charge movement and contractile activation parameters in the same fibre. Such experiments are essential for testing the hypothesis that membrane charge movement is the voltage-sensitive step in the sequence of events leading from fibre depolarization to contractile activation (Schneider & Chandler, 1973). This type of experiment has generally not been feasible with the micro-electrode techniques previously employed because of the risk of fibre damage during contraction.

In the present experiments we have used the single gap method to compare charge movement and contraction thresholds for a variety of depolarizing pulses applied either to normally polarized fibres or to partially depolarized fibres. Our general

conclusion is that the pulse duration required to produce a just-detectable fibre contraction is determined by the time needed to move a set amount of charge. Some of the results have been presented previously in abstract form (Schneider & Horowicz, 1977, 1978, 1979).

METHODS

Single semitendinosus or ileofibularis fibres from cold-adapted *Rana pipiens* were prepared and mounted in a single Vaseline gap chamber using the procedures described in the previous paper (Horowicz & Schneider, 1981). All experiments were carried out using solution C2 in the closed end (C) pool and solution A1 in the open end (A) pool (Table 1 in Horowicz & Schneider, 1981). About 40–60 min were generally allowed for solution equilibration before the fibres were voltage-clamped as previously described. The pulse routines and analysis procedures used for charge movement measurements were as described in the preceding paper. Experiments were carried out at 1–4 °C.

Contraction thresholds and charge moved at threshold

Contraction thresholds were detected by observing the tendon end of the fibre using a compound microscope with a 40× water-immersion objective (Zeiss) and 10× eyepieces (Nikon). A period of about 15 min was allowed following the initial polarization of the terminated segment or following each change in holding potential before making any measurements. A 70 or 100 msec depolarizing pulse was varied in amplitude in 1 mV steps and the smallest pulse producing detectable movement was determined. The membrane potential during this pulse was taken to be the rheobase potential V_{rh} for contraction. The 70 or 100 msec pulse procedure was generally repeated a few minutes later to check for stability. The threshold duration for each of several larger depolarizations of set amplitude was then determined by varying the pulse duration in 1 msec increments for pulses longer than 10 msec or in 0·1 or 0·2 msec increments for pulses shorter than 10 msec. The shortest pulse which reproducibly produced detectable movement at each voltage was taken to be the threshold duration t_{th} for contraction at that voltage. These results constituted a contraction threshold strength–duration curve.

Charge movement currents I_Q were next measured using 100 or 50 msec pulses to each voltage at which t_{th} had previously been determined. I_Q was also measured for 100 msec pulses to voltages within ± 10 mV of V_{rh}. After repeating the pulse sequence for the charge movement measurements four or eight times, which generally required about 10–20 min depending on the number of pulses in the sequence and the amount of averaging, the contraction threshold strength–duration curve was redetermined. Data from fibres exhibiting large drifts in the strength–duration curve were not used.

RESULTS

A. Experiments on fully polarized fibres

Charge moved at contraction threshold

The first experiments were aimed at determining the relationship between charge movement and contraction threshold for pulses to a variety of membrane potentials in normally polarized fibres. Records for one such pulse are presented in Fig. 1. Trace *c* is the V'_m voltage record for a 100 msec pulse from -105 to -45 mV and trace *b* is the charge movement current I_Q which accompanied the pulse. Trace *a* gives the time course $Q(t)$ of charge moved, calculated as the running integral of trace *b*. The vertical dotted line in Fig. 1 marks the pulse duration t_{th} which was just sufficient to produce detectable contraction with a pulse of this amplitude. The charge moved by I_Q up to t_{th} is defined as the threshold charge Q_{th}. Its value lies on the $Q(t)$ trace at the point of intersection with the line marking t_{th}. The total charge Q_{ON} moved by I_Q during the pulse corresponds to the steady level of the $Q(t)$ record during the pulse.

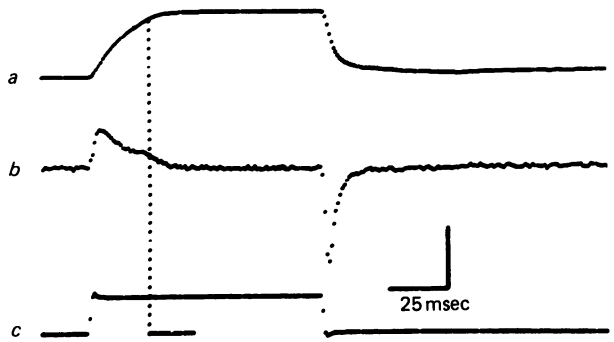

Fig. 1. Method of determining the amount of membrane charge moved during a pulse duration which produced just-detectable contraction. Traces *a*, *b* and *c* give $Q(t)$, I_Q and V'_m for a 100 msec pulse from −105 to −45 mV. This pulse produced substantial contraction. The vertical dotted line marks the pulse duration t_{th} which produced microscopically just-detectable contraction at −45 mV. Responses to eight pulses were averaged to obtain each trace. Calibrations are 25 msec horizontal, and 10 nC/μF (*a*), 1 μA/μF (*b*) or 100 mV (*c*) vertical. Fibre 116, run 1. l_C = 634 μm, s = 2·46 μm, d = 61 μm. Temperature 1·7 °C.

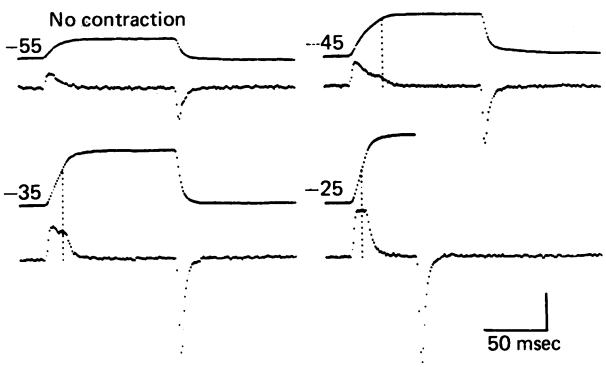

Fig. 2. Charge movement and pulse durations for just-detectable contraction at several membrane potentials. The upper record of each pair is $Q(t)$ and the lower record is I_Q, with the number next to each pair giving V'_m during the pulse (mV). The t_{th} value for each of the three larger pulses is marked by a vertical dotted line. The pulse to −55 mV was below rheobase for contraction. Calibrations are 50 msec horizontal, and 10 nC/μF vertical for $Q(t)$ or 1 μA/μF for I_Q. Same fibre and run as in Fig. 1. Records for the pulse to −45 mV are identical to those in Fig. 1.

Fig. 2 presents I_Q and $Q(t)$ records for the pulse in Fig. 1 and three other pulses in the same fibre, with the voltage during each pulse indicated next to each pair of records. Contraction was produced by each of the three larger pulses but not by the smallest pulse used for Fig. 2. The location of t_{th} for each of the three larger depolarizations is marked by a vertical dotted line. As the depolarization was

increased, t_{th} became shorter. Since the rising phase of $Q(t)$ also became more rapid, the net effect was that Q_{th} remained about constant with increasing depolarization, even though Q_{ON} was steadily growing. The value of Q_{ON} for the smallest pulse in Fig. 2, which was below rheobase for contraction, was less than the Q_{th} values for each of the three larger pulses.

Fig. 3 presents values of Q_{th} and Q_{ON} obtained from a fibre in which the voltage range beyond the rheobase for contraction was explored in relatively small steps. The

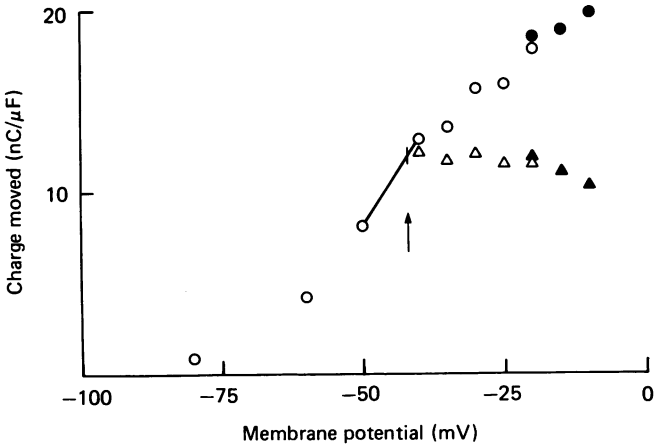

Fig. 3. Voltage dependence of total charge movement and of charge moved during pulse durations which produced just-detectable contraction. Circles give Q_{ON} and triangles give Q_{th} for pulses to the indicated membrane potentials from a holding potential of −100 mV. The vertical arrow marks the membrane potential for just-detectable contraction with a 70 msec pulse. Open symbols denote use of the 100 msec ON analysis routine and filled symbols denote 50 msec ON analyses (Horowicz & Schneider, 1981). Only the two largest pulses were 50 msec in duration. The ON of the largest 100 msec pulse was analysed using both routines. Eight pulses to each potential were averaged for measuring charge movement. Fibre 82. $l_C = 811$ μm, $s = 2{\cdot}56$ μm, $d = 77$ μm. Temperature 1·4 °C.

results are plotted as a function of membrane potential during the pulse. The triangles give the Q_{th} values, obtained as illustrated in Figs. 1 and 2, and the circles give Q_{ON}. The rheobase is marked by the vertical arrow. Here Q_{th} was assumed to equal Q_{ON}, which was approximated by linear interpolation using the two neighbouring Q_{ON} values. Fig. 3 shows that Q_{th} was approximately constant from the rheobase to the largest depolarizations used whereas Q_{ON} increased continuously over the same voltage range. The mean (±S.D.) value of Q_{th} for this fibre was $11{\cdot}6 \pm 0{\cdot}6$ nC/μF.

Strength–duration curves for just-detectable contraction for the fibre in Fig. 3 are presented in Fig. 4. In this case contraction thresholds were determined three times: before starting, half-way through, and following the charge movement measurements. Filled circles denote contraction threshold values which were identical in all three determinations, the half-filled circle denotes values which were identical in two determinations and open circles denote individual values. Fig. 4 shows that contraction thresholds were quite reproducible, with the largest change in t_{th} occurring for the

pulse to a voltage slightly above rheobase. For such a pulse I_Q was quite small near t_{th} so that the variation in t_{th} values resulted in relatively little variation in the values of Q_{th}.

It was convenient for these experiments to measure Q_{th} using pulses much longer than t_{th}. This procedure allowed both total ON and OFF charge to be measured and also allowed calculation of two Q_{th} values for a given voltage for instances when a drift in the threshold duration occurred. In such cases the average of the two values was used as Q_{th}. Integrating I_Q for the threshold duration

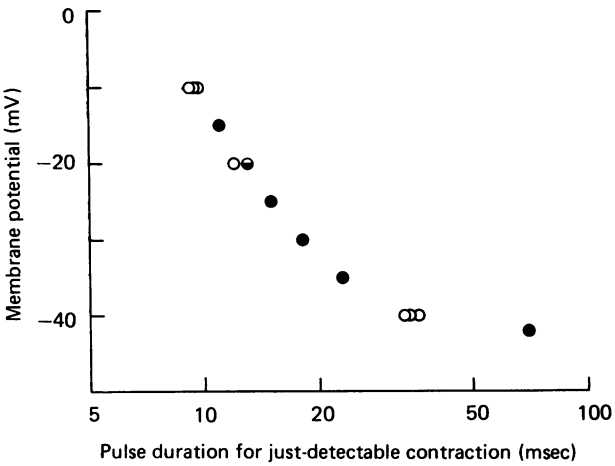

Fig. 4. Strength–duration curve for microscopically just-detectable contraction. Three sets of contraction threshold determinations were made over a period of 68 min. The electrical measurements for the charge movement results of Fig. 3 were interspersed between these contraction threshold determinations. Filled circles mark three identical measurements, the half-filled circle marks two identical measurements and open circles mark individual values. Same fibre and run as in Fig. 3.

may, however, have caused a small systematic underestimate of Q_{th} for the larger pulses where I_Q was still large at the end of the threshold duration (Fig. 2). In such cases, non-instantaneous repolarization due to cable delays both along the fibre and into the T-system may have given rise to a situation where a small additional amount of charge was moved in the ON direction during the first OFF intervals. Such charge should have been included in Q_{th} but was not determined in these measurements.

Different pulses giving threshold contractions move the same amount of charge

The Q_{th} values obtained from fourteen fibres were grouped according to their corresponding t_{th} values and then averaged by group. The resulting relationship between the average Q_{th} and t_{th} values is shown in Fig. 5*A*. It can be seen that Q_{th} was quite independent of t_{th}, with each group average value lying within $\pm 10\%$ (dashed lines) of the overall average Q_{th} value of 11·5 nC/μF (continuous line).

Each point in Fig. 5*A* was obtained from a slightly different subgroup of the overall fibre population. Since the fibre-to-fibre variation in the mean value of Q_{th} was often greater than the variation of Q_{th} values from individual fibres, use of different fibre groups for each point in Fig. 5*A* tended to obscure the actual relationship between Q_{th} and t_{th}. This problem was avoided by first normalizing the Q_{th} values from each

fibre to the mean of the Q_{th} values determined in the same fibre for t_{th} between 10 and 20 msec. The normalized Q_{th} values were then grouped as for Fig. 5*A* and averaged, giving the results shown in Fig. 5*B*. The continuous and dashed lines give mean and $\pm 10\%$ from mean, as in Fig. 5*A*. The standard error for each point in Fig.

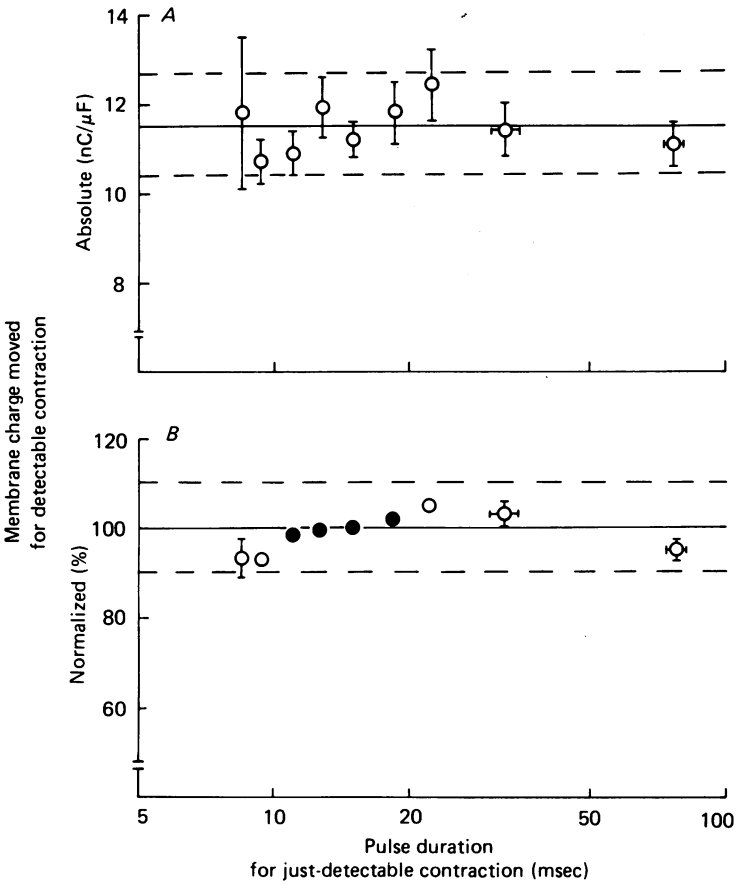

Fig. 5. Average charge moved during pulse durations which produced just-detectable contraction in fourteen fibres. *A*, absolute values of Q_{th} for several different pulses from each fibre were grouped according to t_{th} values and averaged. *B*, same data as in *A* but with the Q_{th} values for each fibre first normalized to the mean value of Q_{th} in that fibre for $10 \leqslant t_{th} \leqslant 20$ msec and then grouped and averaged. The filled circles denote averages of values used for normalization. In both *A* and *B* error bars are ± 1 S.E.M. and absence of error bars indicates that the standard error was smaller than the symbol. Dashed lines mark $\pm 10\%$ from mean (continuous line). $482 \leqslant l_C \leqslant 836\ \mu m$, $2{\cdot}18 \leqslant s \leqslant 2{\cdot}76\ \mu m$, $45 \leqslant d \leqslant 92\ \mu m$. Temperature 1–3 °C.

5*B* was relatively less than in Fig. 5*A*, indicating that fibre-to-fibre variation in the mean value of Q_{th}, which was eliminated from *B* by the normalization process, was indeed a major source of variability. Fig. 5*B* clearly shows that there was very little relative change in Q_{th} over this range of pulse durations. The slight but apparently

reproducible downward trend of Q_{th} with decreasing t_{th} may be attributable to the previously mentioned tendency to underestimate Q_{th} for large short pulses.

Fig. 6*A* presents the average strength–duration relationship for just-detectable contraction obtained from the fibres of Fig. 5. Results were again grouped for

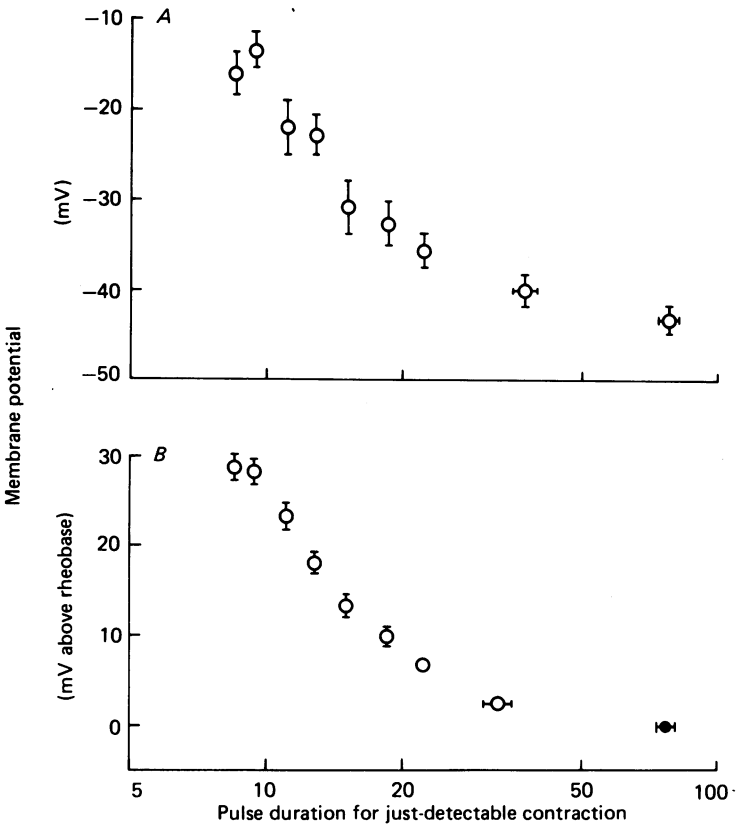

Fig. 6. Average strength–duration curve for just-detectable contraction. Results from the same runs on fourteen fibres as used for Fig. 5. *A*, absolute values of V'_m during each pulse were grouped by t_{th} values and averaged. *B*, same data as in *A* but with the rheobase voltage for contraction subtracted from the membrane potential during each pulse before grouping and averaging. The error bars are as in Fig. 5.

averaging according to t_{th} values so that, as in Fig. 5, each point was determined using a somewhat different fibre subgroup. For Fig. 6*B* voltages for each fibre were first calculated relative to the rheobase voltage for the same fibre and then averaged. This removed any small uncertainties as to absolute voltages and decreased the variability in the average strength–duration curve.

Sub-rheobase prepulses alter contraction threshold pulse durations but do not alter threshold or total charge

The preceding results indicate that the threshold pulse duration for producing detectable contraction is determined by the time necessary to move a threshold quantity of charge, independent of the I_Q time course and amplitude. In order to test this hypothesis further, a series of experiments was carried out in which a given test pulse was used alone or preceded by a prepulse which by itself produced no contraction.

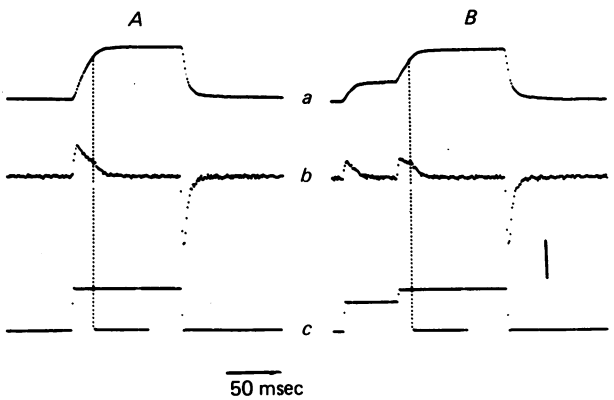

Fig. 7. Procedure for determining the effect of prepulses on the charge moved during pulse durations which produced just-detectable contraction. *A*, traces for a test pulse applied without prepulse. *B*, traces for a prepulse followed by the same test pulse as in *A*. In each part, traces *a* to *c* are $Q(t)$, I_Q and V'_m. The prepulse segments of $Q(t)$ and I_Q in *B* were constructed from the first 50 msec of a 100 msec pulse to the prepulse voltage in the same run, since I_Q base lines for the 50 msec prepulses which preceded the test pulse could not be reliably determined. Responses to eight pulses were averaged to obtain each trace. Calibrations are 50 msec horizontal, and 10 nC/μF (*a*), 1 μA/μF (*b*) or 76 mV (*c*) vertical. Fibre 124, run 2. $l_C = 608$ μm, $s = 2{\cdot}38$ μm, $d = 83$ μm. Temperature 4·0 °C.

Parts *A* and *B* of Fig. 7 present two sets of records from one such experiment. In each part traces *a* to *c* give $Q(t)$, I_Q and V'_m. The records in *A* were obtained with the test pulse without prepulse whereas those in *B* were obtained using the same test pulse immediately preceded by a 50 msec prepulse to a potential below rheobase for mechanical activation. With the prepulse (Fig. 7*B*) the outward membrane charge movement occurred in two phases, one during the prepulse and a second during the test pulse. The I_Q amplitude was smaller during the test pulse which followed a prepulse (Fig. 7*B*, *b*) than during the test pulse applied alone (7*A*, *b*). The total charge Q_{ON} moved by the prepulse plus following test pulse was, however, about the same as the charge moved by the test pulse without prepulse. This is indicated by the similarity of the steady levels of $Q(t)$ during the two test pulses in Fig. 7.

The threshold durations for detectable contraction are indicated by the vertical dotted lines in Fig. 7. The prepulse shortened the test pulse duration t_{th} required to produce contraction. The charge Q_{th} moved at contraction threshold was, however,

about the same with or without prepulse, as seen by the agreement of the intersections of the $Q(t)$ traces with the t_{th} lines in Fig. 7 *A* and *B*.

Sets of superimposed $Q(t)$ records obtained with the two-step experiment in each of two fibres are presented in Fig. 8. Each set of records presents $Q(t)$ for the test pulse alone and for the same test pulse preceded by two different sub-rheobase prepulses. Q_{th} for each record is marked as the intensified point. In each case shown in Fig. 8, Q_{th} was about the same with or without prepulses, despite the marked

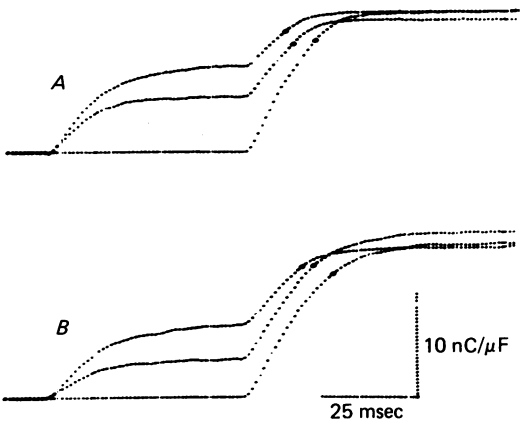

Fig. 8. Effect of prepulses on total charge movement and on the charge moved during pulse durations which produced just-detectable contraction. Traces give $Q(t)$ for a test pulse applied either alone or immediately following each of two 50 msec prepulses to voltages below rheobase for contraction. Each intensified point shows the charge moved at t_{th}. Prepulse segments were constructed as in Fig. 6. Eight pulses were averaged for each record. *A*, run 1 on the fibre shown in Fig. 7. *B*, fibre 120, run 5. $l_C = 636$ μm, $s = 2{\cdot}71$ μm, $d = 54$ μm. Temperature 1·9 °C.

differences in the $Q(t)$ time course introduced by the prepulses. This is consistent with the hypothesis that t_{th} is determined by the time required to move a threshold amount of charge, independent of the $Q(t)$ time course.

Table 1 summarizes the results of all two-step experiments. As shown in Fig. 8, each test pulse was used alone and together with two different sub-rheobase prepulses. The charge Q_{ON} moved during each prepulse and each test pulse is given in columns 5 and 6 of Table 1. Column 7 gives the ratio of the sum of Q_{ON} for each prepulse–test pulse combination to the Q_{ON} for the same test applied alone. The ratios are close to unity, with the mean $\pm$ S.E. of all runs being $0{\cdot}97 \pm 0{\cdot}03$. The amount of total charge moved at the end of the test pulse was thus independent of whether or not the test pulse was preceded by prepulses which moved on average 42 ± 4% of the total available pulse Q_{ON}.

Average values of t_{th} for the test pulses without and with prepulses are given in column 8 of Table 1. Preceding the test pulse by the larger prepulses decreased t_{th} by 5·8–7·8 msec. The t_{th} values were used to calculate the component of threshold charge moved during each test pulse, giving the results in column 9. When the test pulse

TABLE 1. Effects of sub-rheobase prepulses on charge movement and threshold pulse durations for contraction

(1) Fibre	(2) Run	(3) V'_m (mV) Test	(4) V'_m (mV) Pre*	(5) Q_{ON} (nC/μF) Pre†	(6) Q_{ON} (nC/μF) Test	(7) Q_{ON} (nC/μF) Pre+test / Control test	(8) t_{th} (msec) Test	(9) Q_{th} (nC/μF)‡ Test	(10) Q_{th} (nC/μF)‡ Pre+test / Control test
120	1	−42	(−106)	—	14·5	—	18·8	10·0	—
			−66	3·0	9·2	0·84	14·0	5·6	0·86
			−56	5·1	6·1	0·78	12·5	3·6	0·87
	5	−42	(−106)	—	14·8	—	23·8	12·0	—
			−66	3·7	12·2	1·08	19·0	9·1	1·07
			−56	7·1	7·4	0·98	16·0	5·7	1·06
	6	−32	(−106)	—	18·5	—	15·8	12·6	—
			−66	3·4	15·3	1·01	12·5	9·4	1·01
			−56	6·4	10·5	0·91	10·0	5·8	0·97
123	1	−30	(−100)	—	13·7	—	26·2	11·5	—
			−50	6·4	9·2	1·14	20·0	6·7	1·13
			−40	8·4	5·6	1·02	19·0	4·2	1·09
124	1	−32	(−102)	—	13·6	—	19·0	11·0	—
			−52	5·4	7·4	0·94	13·0	5·2	0·97
			−42	8·4	5·3	1·00	11·5	3·6	1·10
	2	−32	(−102)	—	13·5	—	19·8	10·7	—
			−52	5·1	8·3	0·98	13·5	5·4	0·98
			−42	7·4	5·3	0·94	13·0	3·9	1·06
Mean ±S.E.M.						0·97 ±0·03			1·02 ±0·03

'Pre' or 'Test' denote the value of the indicated parameter for the prepulse or test pulse. 'Control test' refers to the value obtained using the test pulse by itself without any prepulses.

* Values in parentheses give holding potentials and indicate test pulses applied without any prepulse.

† In order to obtain an accurate value for the charge moved by the prepulse it was applied alone and the Q_{ON} and Q_{OFF} values were averaged to give the values tabulated here.

‡ The 'Test' value of Q_{th} gives the charge moved during t_{th} at the test pulse membrane potential. The 'Pre' value of Q_{th} is equal to the entire Q_{ON} for the prepulse.

was preceded by a prepulse, the total threshold charge consisted of the entire charge moved during the prepulse plus the component moved during t_{th} of the test pulse. The ratio of this sum to Q_{th} for the test pulse without prepulse is given in column 10 of Table 1. In all cases the ratio was close to unity, with the mean of all runs being $1{\cdot}02 \pm 0{\cdot}03$. Thus Q_{th} was the same whether or not the test pulse was preceded by prepulses, which moved on average $51 \pm 4\%$ of the total Q_{th}.

B. Charge movement and contraction thresholds during steady partial depolarization

In both the single- and double-step experiments contraction threshold coincided with the time needed to move a set amount of charge. Since prolonged partial depolarization depresses contractile activity (Hodgkin & Horowicz, 1960) and decreases membrane charge movement (Chandler *et al.*, 1976*b*; Adrian & Almers, 1976), it was of interest to determine whether partial depolarization altered the amount of charge moved at contraction threshold.

Steady partial depolarization shifts the contraction threshold strength–duration curve

Fig. 9 presents contraction threshold strength–duration curves obtained in one experiment. Each circle gives the average result of strength–duration measurements made before and after a charge movement run at a holding potential V_H of -96 mV. A total of four different paired strength–duration determinations and associated charge movement measurements were made at the -96 mV holding potential over a period of more than 6 hr. The remarkable stability of this fibre is indicated by the small variation in the four strength–duration curves for V_H of -96 mV. A single strength–duration curve determined after shifting V_H to -116 mV for 15 min (diamonds in Fig. 9) agreed with the curves for $V_H = -96$ mV, thus showing that contractile ability was fully primed at -96 mV.

Between each set of measurements at the -96 mV holding potential, V_H was changed to a depolarized level and the strength–duration and charge movement measurements were carried out at the new holding potential. At least 14 min were allowed following each change in V_H before making any measurements. All pulses for determining strength–duration curves or charge movement in partially depolarized fibres were applied 50 msec after a step back to the fully polarized holding potential, as shown in trace *c* of Fig. 10*B*. This step was too short to restore any significant amount of inactivated charge (Chandler *et al.* 1976*b*), but did provide for the use of identical pulses for the charge and threshold measurements in both the fully polarized and partially depolarized conditions. It should also have allowed any sub-threshold build-up of myoplasmic free calcium, $[Ca]_i$, to be restored approximately to the fully polarized level, since following small depolarizations the time constants for decline of $[Ca]_i$ under generally similar conditions are about 15–20 msec (Kovács, Ríos & Schneider, 1979).

In the fibre of Fig. 9 two runs were carried out at a V_H of -66 mV and a single run at -56 mV, with each bracketed by runs made with V_H returned to -96 mV. The squares in Fig. 9 present strength–duration results for the two runs at $V_H = -66$ mV. The 30 mV steady depolarization elevated the threshold voltage for the 70 msec pulse and increased t_{th} for each of the larger pulses. The effect was fully reversible and quite reproducible.

The triangle with upward arrow in Fig. 9 indicates that in the run in which V_H was set at the further depolarized level of −56 mV, no movement was detected for 100 msec pulses to +16 mV. Following this run a return to $V_H = -96$ mV gave the original strength–duration relationship, demonstrating complete reversibility of the abolition of contraction.

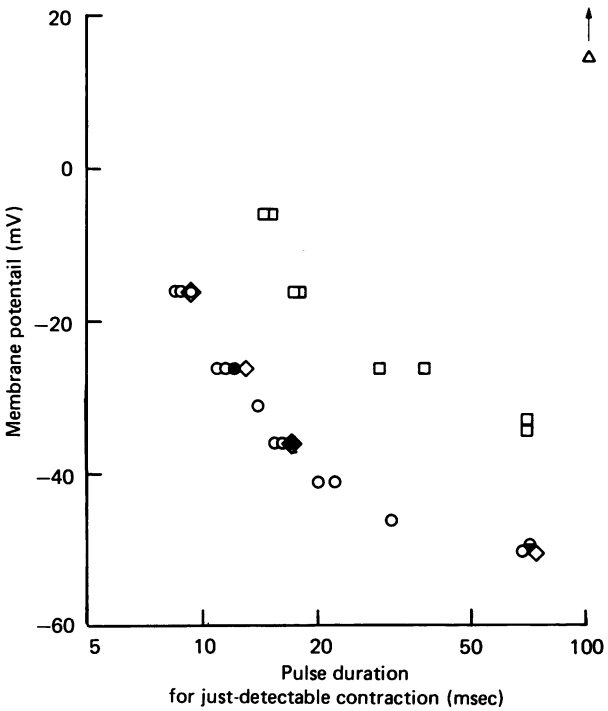

Fig. 9. Effect of steady partial depolarization on the strength–duration relationship for just-detectable contraction. ○, ◒, ●: $V_H = -96$ mV, runs 2, 5, 8 and 10. ● denotes two identical values and ◒ denotes three identical values. Single circles at a given potential are from run 2, double circles from runs 2 and 5 and triple circles from runs 5, 8 and 10. ◇: $V_H = -116$ mV, determined between runs 8 and 9 and not accompanied by electrical measurements. □: $V_H = -66$ mV, runs 4 and 6. △: $V_H = -56$ mV, run 9 (upward arrow indicates no contraction detected). Fibre 89. $l_C = 684\ \mu m$, $s = 2{\cdot}46\ \mu m$, $d = 45\ \mu m$. Temperature 2·2–2·7 °C.

Steady partial depolarization decreased membrane charge movements

Two sets of $Q(t)$, I_Q and V'_m records from the fibre of Fig. 9 are presented in Fig. 10. For part *A* of Fig. 10 V_H was −96 mV whereas for part *B* V_H was −66 mV. In both parts the depolarizing pulse (traces *c*) covered the identical voltage range since for *A* it was applied from the holding potential whereas for *B* it was preceded by a 50 msec hyperpolarizing step to −96 mV. The vertical dotted lines in Fig. 10 mark t_{th} for the two pulses and demonstrate the lengthening of t_{th} as a result of steady partial depolarization. Fig. 10 also shows that in the partially depolarized state $Q(t)$ and I_Q (traces *a* and *b* of part *B*) were depressed compared with the corresponding records obtained under full fibre polarization (part *A*).

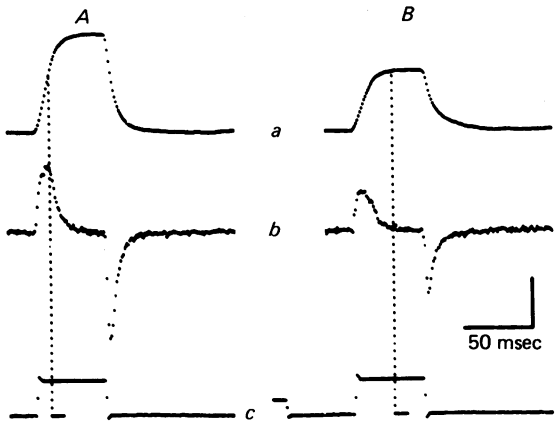

Fig. 10. Procedure for determining the effect of steady partial depolarization on the charge moved during pulse durations which produced just-detectable contractions. *A*, $V_H = -96$ mV. *B*, $V_H = -66$ mV. Traces *a*, *b* and *c* in both *A* and *B* give $Q(t)$, I_Q and V'_m. In *B* a 50 msec prepulse to -96 mV directly preceded the same depolarizing pulses to -26 mV as used in *A*, so that the $Q(t)$ and I_Q traces in *A* and *B* are for identical pulses. Recording started 20 msec before the depolarizing pulse. The initial 40 msec of the V'_m trace in *B* was not recorded but was constructed for the purpose of illustration by appropriately scaling and moving the OFF segment of V'_m in the same trace. Same fibre as in Fig. 9.

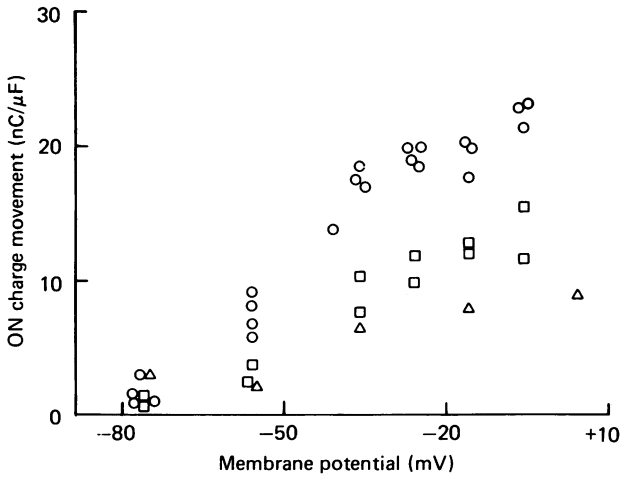

Fig. 11. Effect of steady partial depolarization on total charge movement. Same fibre as in Figs. 9 and 10. Circles, squares and triangles give Q_{ON} values at $V_H = -96$, -66 and -56 mV from the same runs as in Fig. 9. The single circle at -41 mV is from run 2 and the three circles at -36, -16 and -6 mV are from runs 5, 8 and 10. To avoid crowding, points determined at the same membrane potential were slightly displaced horizontally in a few cases.

Charge movement results from this experiment are presented in Fig. 11 in the form of a graph of Q_{ON} *vs.* voltage during the pulse. Results of each of the control runs at −96 mV are given by the circles. The good agreement of results of repeat runs indicates minimal change in charge movement for the fully polarized condition over the course of the experiment. The two sets of squares and single set of triangles in Fig. 11 give the total ON charge respectively for the two runs at $V_H = -66$ mV and single run at $V_H = -56$ mV. Prolonged depolarization reproducibly and reversibly

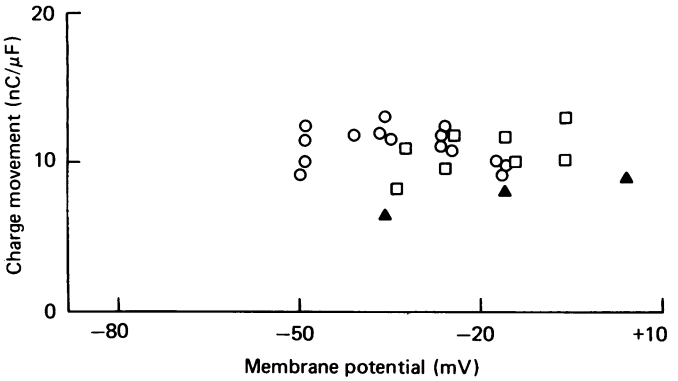

Fig. 12. Effect of steady partial depolarization on charge moved during pulse durations which produced just-detectable contraction. Same fibre as in Figs. 9 to 11. Circles and squares give Q_{th} values at $V_H = -96$ and −66 mV, corresponding to the t_{th} values in Fig. 9. The filled triangles give Q_{ON} at $V_H = -56$ mV from run 9, during which no contraction was detected.

depressed Q_{ON}. For pulses to −36 mV and beyond, the average value of Q_{ON} relative to the bracketing control measurements at $V_H = -96$ mV was 52 % for one run with $V_H = -66$ mV and 64 % for the other. The further depolarization to $V_H = -56$ mV (triangles in Fig. 11), which totally eliminated contraction, further decreased Q_{ON} to 39 % of the bracketing control levels for pulses to and beyond −36 mV.

Charge moved at contraction thresholds was only slightly decreased by steady partial depolarization

Values of Q_{th} for the fibre in Figs. 9–11 are presented in Fig. 12. The circles give Q_{th} as a function of membrane potential during the pulse for the four runs at $V_H = -96$ mV. As previously discussed, Q_{th} in the fully polarized condition was relatively constant over the range of pulse voltages examined. The two sets of squares in Fig. 12 give Q_{th} for the two runs in which V_H was −66 mV. In both these partially depolarized runs Q_{th} was also found to be relatively independent of pulse voltage. The mean of the Q_{th} values, each expressed relative to the average Q_{th} for the bracketing control runs, was 86 % for the first run and 103 % for the second run at $V_H = -66$ mV. Thus Q_{th} was only minimally depressed by changes in holding potential which decreased the total ON charge to 52 % and 64 % of control. This was due to the lengthening of t_{th} in the partially depolarized state, as shown in Figs. 9 and 10.

When the fibre in Figs. 9 to 12 was further depolarized to $V_H = -56$ mV, no movement was observed for 100 msec pulses to +16 mV. Under the hypothesis that contraction threshold is determined by the time required to move Q_{th} the absence of contraction should indicate that Q_{ON} was less than Q_{th}. The Q_{ON} values for each of the three largest pulses used with the −56 mV holding potential are replotted from Fig. 11 as filled triangles in Fig. 12 and do indeed fall below the Q_{th} values obtained at the V_H levels of either −96 or −66 mV.

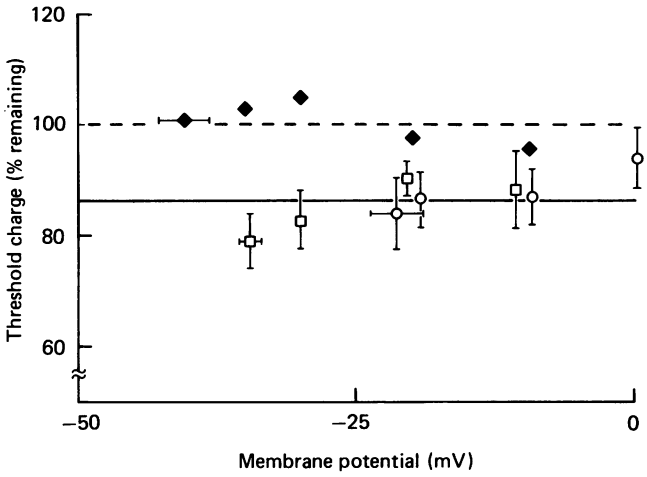

Fig. 13. Average fractional threshold charge remaining during steady partial depolarization. Ten runs during partial depolarization were separated into two groups according to rheobase membrane potential for contraction. Open squares, group I (runs 4 and 6 on fibre 89, run 2 on 91 and runs 3 and 4 on 113). Open circles, group II (run 3 on fibre 91, run 7 on 93, run 6 on 96 and runs 6 and 7 on 113). See Table 2 for run data. Vertical error bars mark ±1 S.E.M. for the average results for groups I and II and horizontal error bars mark ±1 S.E.M. for the average rheobase voltages. The continuous horizontal line marks the average of all fractional remaining Q_{th} values from both groups I and II, and the dashed horizontal line marks unity. Filled diamonds, average values for the bracketing fully polarized runs. $608 \leqslant l_C \leqslant 836$ μm, $2{\cdot}18 \leqslant s \leqslant 2{\cdot}64$ μm, $45 \leqslant d \leqslant 77$ μm. Temperature 1–3 °C.

Fractions of total and threshold charges remaining during partial depolarization

The partial inactivation experiments were in general rather difficult to complete successfully because of drift in contraction thresholds during partial depolarization. We did, however, manage to obtain eleven successful runs in the partially depolarized but still contracting condition, each bracketed by runs with similar strength–duration curves in the fully polarized state. One of these runs was suspect since (i) the observer noted during the experiment that the threshold contractions at full polarization seemed stronger than usual and (ii) the strength–duration curve at partial depolarization was essentially the same as at full polarization. This run was eliminated from further consideration.

The ten remaining runs during steady partial depolarization, which involved five different fibres, were separated into two groups according to the membrane potentials

at rheobase, V_{rh}. Using primed symbols to denote parameter values under partial depolarization, each Q'_{th} value was expressed as a fraction $Q'_{th}/\bar{Q}_{th}$ of the average, $\bar{Q}_{th}$, of Q_{th} values for all pulses in the two runs at full polarization which bracketed a partially depolarized run. Average values of $Q'_{th}/\bar{Q}_{th}$ for the two groups of partially depolarized runs are plotted in Fig. 13 as a function of membrane potential during the pulse. The squares (group I) are average results for five runs (three fibres) having V_{rh} between -38 and -32 mV, and the circles are average results for five runs (four

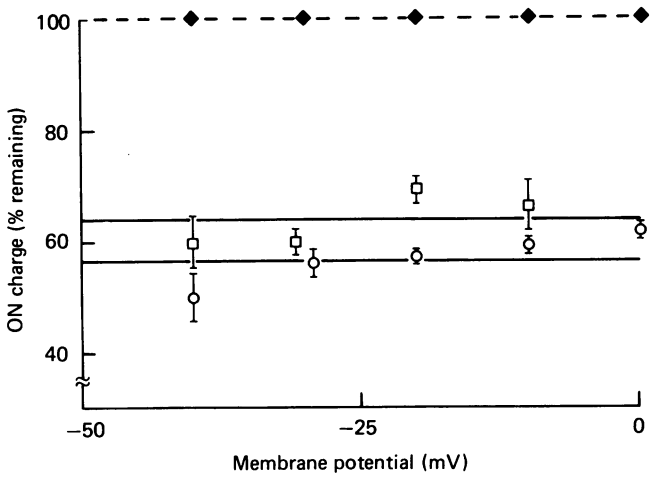

Fig. 14. Average fractional total ON charge remaining during steady partial depolarization. Symbols denote averages (±1 S.E.M.) for the same fibre groupings as in Fig. 13. Upper and lower continuous horizontal lines mark the average fractional remaining Q_{ON} values for groups I and II respectively.

fibres) having V_{rh} between -26 and -12 mV. The left-most square and circle give the average rheobase voltage and average $Q'_{th}/\bar{Q}_{th}$ at rheobase for each group. For both groups $Q'_{th}/\bar{Q}_{th}$ remained roughly constant for pulses increasingly beyond rheobase, as is the case for Q_{th} in fully polarized fibres. All average Q'_{th} values were slightly less than $\bar{Q}_{th}$ for the fully polarized condition. For all measurements in group I the average (±S.D.) $Q'_{th}/\bar{Q}_{th}$ was $0{\cdot}85 \pm 0{\cdot}11$ and for group II it was $0{\cdot}88 \pm 0{\cdot}10$. The continuous horizontal line in Fig. 13 marks the overall average $Q'_{th}/\bar{Q}_{th}$ for both groups, which was $0{\cdot}86 \pm 0{\cdot}11$. For comparison, the filled diamonds give the average values of $Q_{th}/\bar{Q}_{th}$ for the bracketing fully polarized runs and the dashed horizontal line marks their mean, which by definition is 1·00.

The average values of Q'_{ON}/Q_{ON} for the two groups of partially depolarized runs are plotted in Fig. 14. Q_{ON} was clearly depressed relatively more than Q_{th} (see Fig. 13), the average (±S.D.) fractional remaining Q_{ON} being $0{\cdot}60 \pm 0{\cdot}08$ as compared with 0·86 for Q_{th}. Fig. 14 also shows that the runs in group II, which were characterized by having more positive V_{rh} values than those for group I, had slightly smaller Q'_{ON}/Q_{ON} values than the group I runs. The overall average values of Q'_{ON}/Q_{ON} for each of the two groups were $0{\cdot}64 \pm 0{\cdot}09$ and $0{\cdot}57 \pm 0{\cdot}07$ and are marked respectively

by the upper and lower continuous horizontal lines in Fig. 14. The diamonds mark the reference levels of fractional remaining Q_{ON} under full polarization, which are all unity (dashed line) since Q_{ON} was normalized separately for each pulse potential.

Note that different normalization procedures were used for Figs. 13 and 14. The threshold charges in Fig. 13 were normalized to the mean of the Q_{th} values for all pulses under full polarization. Such a procedure was used in order to study the voltage dependence of Q'_{th} independent of any possible minor voltage dependence of Q_{th}.

TABLE 2. Fractional remaining charge movement during steady partial depolarization

(1) Fibre	(2)* Run	(3) V_H (mV)	(4) Q'/Q	(5) $Q'_{th}/\bar{Q}_{th}$	(6)† Q'_{lin}/Q_{lin}
89	4	−66	0·52	0·86	1·00
	6	−66	0·65	1·03	0·98
91	2	−70	0·68	0·78	1·07
	3	−60	0·54	0·89	1·00
93	7	−64	0·57	0·78	0·94
96	3	−65	0·61‡	0·80‡	1·03‡
113	3	−65	0·71	0·79	0·98
	4	−60	0·64	0·80	1·00
	6	−55	0·56	0·98	0·99
	7	−55	0·52	0·98	1·01
Mean ± S.E.M.			0·60 ±0·02	0·87 ±0·03	1·00 ±0·01

Each entry in columns 4–6 is the mean of the ratios of the value of the parameter during the indicated partially depolarized run to its average value in two bracketing runs in the fully polarized condition.

* Sequential runs shared the same bracketing fully polarized controls.

† Q_{lin} and Q'_{lin} are the areas of the 'mean linear' capacitative current transient for hyperpolarizing pulses (Horowicz & Schneider, 1981) in fully polarized and partially depolarized runs.

‡ When fibre 96 was partially depolarized the OFF segment of the 'mean linear' record for hyperpolarizing pulses could not be corrected by the standard procedure of using a linearly sloping base line. In this case an exponential function of time was fitted to the latter part and subtracted from the entire 'mean linear' OFF. The remaining transient was used to remove linear capacitative current from depolarizing pulse ON and OFF currents. Straight sloping base lines were used as usual after removing the linear capacitative current. This special analysis gave essentially the same results as the standard linear base-line analysis when applied to a fully polarized run on the same fibre.

Table 2 summarizes the partial depolarization experiments. Column 4 gives the average Q'_{ON}/Q_{ON} for each partially depolarized run and column 5 gives the average $Q'_{th}/\bar{Q}_{th}$. In all cases $Q'_{th}/\bar{Q}_{th}$ was greater than Q'_{ON}/Q_{ON}.

Charge movement during partial depolarization sufficient to eliminate contraction

Three runs were carried out on two of the fibres in Table 2 using slightly more depolarized holding potentials which were sufficiently low to eliminate contraction completely. In these runs, which are not included in Table 2, Q_{ON} was decreased to 30–45% (mean = 41%) of its value in the bracketing fully polarized runs. The maximum value of Q_{ON} in each of these runs averaged 77% of the Q_{th} values determined in the bracketing fully polarized control runs. Using this result and the

fractional remaining Q_{th} values for partially depolarized but still-contracting fibres, a total charge movement of greater than 77 % but not more than 87 % of the Q_{th} value under full polarization appears to be required to produce contraction of fibres experiencing steady partial depolarization.

Linear capacitance is unchanged during steady partial depolarization

Steady partial depolarization which depressed but did not eliminate contractile activity had no effect on the linear fibre capacitance measured using hyperpolarizing pulses from −100 mV. This is shown by column 6 of Table 2, which gives the ratio of the charge Q_{lin} carried by the 'mean linear' capacitative transient (Horowicz & Schneider, 1981) to the average of the Q_{lin} values for each bracketing run at full polarization. These ratios were in all cases close to unity, with the mean (±S.E.) of all measurements being 1·00±0·01. It is thus clear that in the present experiments the effects of steady partial depolarization cannot be attributed to changes in linear fibre capacitance.

C. Charge movement kinetics

It has been previously reported that charge movement currents exhibit bumps and notches for pulses to about −50 to −20 mV (Almers, Adrian & Levinson, 1975; Adrian & Peres, 1977; Adrian, 1978). We have observed such bumps and notches in I_Q records both from contracting fibres and from fibres in which contraction was blocked by 20 mM-internal EGTA (Horowicz & Schneider, 1981). Since the bumps and notches may indicate the presence of an additional component of I_Q, it was of interest to determine when they occurred relative to t_{th}. It was also of interest to see how the I_Q ON kinetics were affected by prepulses and by steady partial depolarization.

Charge movement kinetics and contraction threshold pulse durations

Fig. 15 presents ON I_Q records for pulses to membrane potentials close to the rheobase for contraction. The number next to each record gives the membrane potential during the pulse, and the vertical cross-lines on each of the four lower records situate t_{th} at the indicated potentials. The upper two records were obtained using pulses which produced no detectable contraction. Within the noise of the traces, the records without movement appear to be characterized by a smoothly declining I_Q. As the pulse was made increasingly to exceed rheobase, first a prolonged tail, then a shoulder and then a definite notch and second peak or bump appeared on the I_Q records. If the tail, shoulder and bump are indicative of another, slower I_Q component, Q_{th} for the fibre of Fig. 15 must have included a small amount of such a component. Results from this and other fibres indicate that the end of the threshold pulse duration for just-detectable contraction either roughly coincided with or occurred slightly later than the start of the shoulders and bumps.

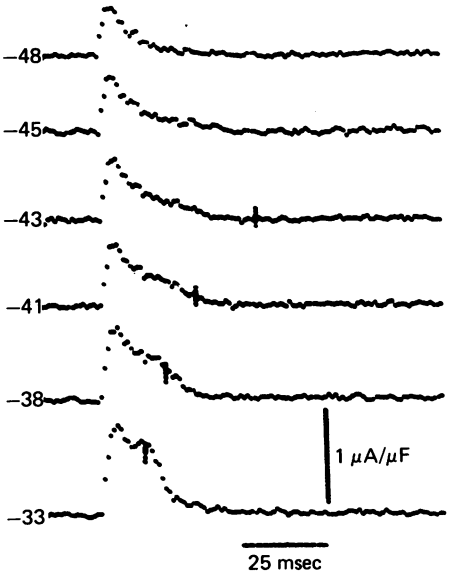

Fig. 15. Charge movement ON kinetics in relation to pulse durations which produced just-detectable contractions. Traces give I_Q during pulses to the indicated membrane potentials (mV). The vertical cross-lines mark t_{th} for the four largest depolarizing pulses. The two smaller pulses went to potentials below the rheobase for contraction. Fibre 79. $l_C = 634$ μm, $s = 2{\cdot}56$ μm, $d = 73$ μm. Temperature 1·3 °C.

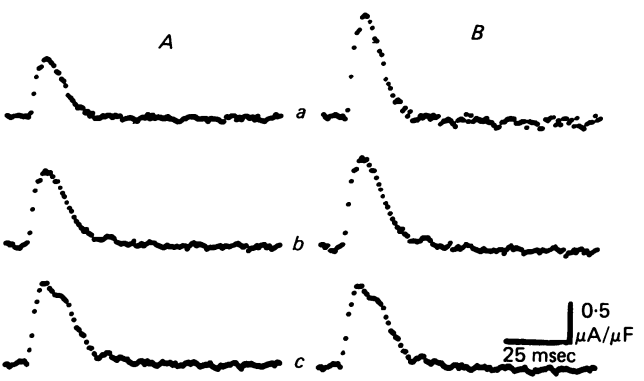

Fig. 16. Effect of prepulses on the charge movement kinetics at a given test pulse membrane potential. All records are for a step to −32 mV. For *c* the step was applied from the −106 mV holding potential, whereas for *b* or *a* the step was directly preceded by a 50 msec prepulse to −66 (*b*) or −56 mV (*a*). Both prepulses were below rheobase for contraction. *A*, I_Q traces as actually recorded. *B*, I_Q scaled by 1·76 (trace *a*) and 1·21 (*b*), making the area under the scaled *a* and *b* traces equal to the area under the unscaled trace *c*. Fibre 120, run 6. Same fibre as in Fig. 8*B*.

Sub-rheobase prepulses selectively depressed the initial phase of test pulse charge movement

Prepulses which are below rheobase for contraction have already been shown to decrease the charge moved during an immediately following test pulse, without altering the total amount of charge moved by prepulse plus test pulse. Figs. 16 and 17 present an attempt to investigate the effect of such prepulses on the test pulse I_Q time course.

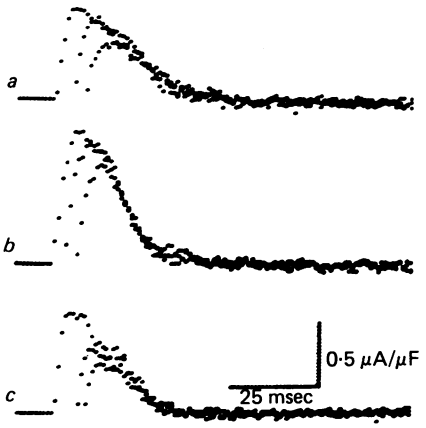

Fig. 17. Effect of sub-rheobase prepulses on charge movement ON kinetics. Each set of I_Q traces is for a step to the same membrane potential. For the larger trace in each set the step was applied from the holding potential, whereas for each of the smaller traces the step was preceded by a 50 msec prepulse to below rheobase for contraction. Each smaller trace was shifted along the time axis by an amount equal to the difference between t_{th} without and with the prepulse. The time shifts were 5 and 8 msec for the traces in *a*, 3 and 6 msec in *b* and 6 and 8 msec in *c*. See Table 1 for prepulse and test pulse membrane potentials. Sets *a* and *b*: fibre 120, runs 5 and 6 (same fibre as in Figs. 8*B* and 16). Set *c*: fibre 124, run 1 (same fibre as in Figs. 7 and 8*A*).

All the I_Q records in Fig. 16 were recorded for a pulse to the same membrane potential, either without prepulse (*c*) or with increasingly large prepulses (*b* and *a*) to potentials below rheobase for contraction. Part *A* of Fig. 16 presents the actual traces and shows the decrease in test pulse I_Q produced by the prepulse. Part *B* indicates that I_Q was not only decreased but that its time course was also altered by the prepulses. To show this, records *a* and *b* of part *A* were scaled up so that each included an area equal to the area under record *c*. The scaled records, presented as *a* and *b* of part *B* of Fig. 16, clearly have time courses different from I_Q for the test pulse without prepulse (record *c*).

Given that I_Q may be composed of two or more components, the possibility that sub-rheobase prepulses selectively mobilized only part of one I_Q component which occurs early in the test pulse was explored. Each panel in Fig. 17 presents three unscaled I_Q records for pulses to the same test pulse membrane potential, one without a prepulse and two with different amplitude sub-rheobase prepulses. Each record obtained after a prepulse was shifted along the time axis to later times so that its

t_{th} coincided with t_{th} for the test pulse without prepulses. After shifting and ignoring the initial rising phases, each I_Q after a prepulse was approximately coincident with the later part of I_Q for the test pulse without prepulse. The prepulses thus appear to have moved the charge which normally would have moved initially during the test pulse without affecting the later phase of test pulse charge movement.

D. A model for charge movement and just-detectable contraction

To guide interpretation and to systematize analysis, it is helpful to work with the preceding results in the context of a plausible model. The challenge of producing one arises from the fact that, with current information, there is considerable choice in selecting possible mechanisms which might underlie the observed relations between charge movements and contractile threshold. In this situation, one approach is to formulate a general model which is comparatively simple in the sense of being able to accommodate most of the observations with a minimum number of variables and parameters and yet which is capable of further development or revision as information accumulates and the need arises. For a mathematical model at any definite stage of development to be adequate, the values of the variables and parameters should be capable of being determined from the data obtained under various experimental conditions.

Two components of charge movement

In generating the mathematical form of the model, two reactions are assumed to contribute to the measured charge movements: reaction A is rate-limiting, with rate constants dependent on membrane potential, while reaction B is rapid and controlled by the degree of advancement of A. Activation of contraction is assumed to be determined by the extent of reaction B, threshold being specified by a fixed amount of this reaction.

Reaction A can be envisaged as consisting of charged groups or dipoles distributing between two positions within the membrane. When the internal potential is negative and has a value near the resting membrane potential the charged groups are mostly found in one position which, from its functional role, can be designated as the standby position. When the membrane is depolarized the charged groups tend to move into the other position, which can be designated as the initiator position. At any given time the fraction of charged groups in the initiator position will be denoted by the variable u, which can take on values between 0 and 1. As the groups move from the standby to the initiator position due to membrane depolarization, a certain amount of charge displacement is produced in the membrane which can be measured by an external circuit. The measured charge displacement due to this reaction in the external circuit, Q_A, is assumed to be proportional to the change in the fraction of groups in the initiator position. If the initial condition is such that $u = 0$, then

$$Q_A = K_A u. \tag{1}$$

The proportionality constant, K_A, is a product of the total number of charged groups present and the charge displacement produced in the measuring circuit by a single group moving from the standby to the initiator position.

Reaction B is assumed to generate rapidly an additional charge displacement and

to be governed by a power function of the fraction of the charged groups of reaction A in the initiator position. Specifically, the charge displacement Q_B measured in the external circuit due to reaction B is given by the relation

$$Q_B = K_B u^n, \tag{2}$$

where n is a positive integer greater than 1 and K_B is a proportionality constant analogous to K_A. Since reaction B is considered to be rapidly reversible and strongly coupled to A it is instantaneously governed by the degree of advancement of reaction A, as measured by the variable u.

The total charge displacement, Q, produced by the two coupled reactions is thus given by

$$Q = Q_A + Q_B = K_A u + K_B u^n. \tag{3}$$

For convenience, eqn. (3) will be rewritten as

$$Q = K(u + Ru^n), \tag{4}$$

where $K = K_A$ and $R = K_B/K_A$. The variable u is a function of membrane potential and time, while R and n are constants. As will be seen below, K depends on the holding potential but is assumed constant for potential pulses of duration less than a few tenths of a second.

Contraction thresholds under full and partial polarization

At this point, the model can be shown to behave qualitatively in accord with the results on contraction thresholds. In fully polarized fibres the time to move a set amount of charge corresponded with the pulse duration required for just-detectable contraction. If threshold is achieved only when reaction B proceeds to a fixed extent independent of the degree of inactivation, then the second term on the right-hand side of eqns. (3) and (4) is constant at threshold, i.e.

$$KRu_{th}^n = Q_{B\,th} = \text{constant}, \tag{5}$$

where u_{th} is the fractional degree of advancement of the first reaction at threshold. The overall charge movement measured at threshold for the two reactions is given by

$$Q_{th} = K(u_{th} + Ru_{th}^n). \tag{6}$$

From eqn. (5),

$$u_{th} = \left(\frac{Q_{B\,th}}{KR}\right)^{1/n}. \tag{7}$$

Eqns. (5) to (7) give

$$Q_{th} = \left(\frac{K^{n-1} \cdot Q_{B\,th}}{R}\right)^{1/n} + Q_{B\,th}. \tag{8}$$

Since K is constant in fully polarized fibres, eqn. (8) shows that the condition that $Q_{B\,th}$ be constant is sufficient to ensure that the overall threshold charge Q_{th} will also be constant in fully polarized fibres, as was observed.

When fibres were partially inactivated by steady partial depolarization, the total amount of charge moved was decreased by about the same percentage for pulses to

each test potential (Fig. 14). The model will account for this observation by assuming that only K is changed by inactivation, so that the currents calculated for charge movement will simply be scaled down by a constant factor at each test potential. In terms of the interpretation given to the model this means that a certain number of charged groups in reaction A are diverted into an inactive and unavailable state. In partially inactivated fibres a set amount of charge movement still determined the contraction threshold, but the amount required was observed to be slightly less than in the fully primed condition. It was assumed that $Q_{B\,th}$ has the same constant value under both full polarization and steady partial depolarization. Since K decreases with steady partial depolarization, eqn. (8) shows that Q_{th} will decrease with steady depolarization if n is greater than 1, but that the fractional decrease of Q_{th} will be less than the fractional decrease of K. This agrees with the experimental results in partially inactivated fibres.

Model parameter values determined from the effects of steady partial depolarization

Estimates of the values of u_{th}, R and K can be obtained from the behaviour of Q_{th} and Q as fibres are inactivated by maintained depolarization. We shall consider a state of steady partial depolarization in which pulse durations for just-detectable contraction are increased. Charge measurements in this partially depolarized state will be compared with those in the fully polarized condition which will be denoted by eqns. (4) to (8). Using primed symbols to denote parameter values for the partially depolarized state, eqn. (4) can be written:

$$Q' = K'[u + R(u)^n], \tag{9}$$

since K and u_{th} are the only parameters changed by inactivation. The threshold condition given by eqn. (5) becomes

$$Q_{B\,th} = K'R(u'_{th})^n = \text{constant}, \tag{10}$$

and eqn. (6) becomes

$$Q'_{th} = K'[u'_{th} + R(u'_{th})^n]. \tag{11}$$

Equating the expressions for $Q_{B\,th}$ in eqns. (5) and (10), one obtains

$$(u_{th}/u'_{th})^n = K'/K. \tag{12}$$

The ratio of eqn. (9) to eqn. (4) gives

$$(K'/K) = (Q'/Q), \tag{13}$$

so that

$$(u_{th}/u'_{th})^n = Q'/Q. \tag{14}$$

(Q'/Q) is the ratio of the overall charge displacement in the partially depolarized state to that in the fully primed state, both measured with pulses to the same membrane potential. In partially inactivated fibres the membrane potential was restored briefly (*ca.* 50 msec) to the holding potential used in the fully primed condition (*ca.* -100 mV) before the pulses for charge and t_{th} measurements were applied. With this type of pulse protocol, (Q'/Q) is independent of the membrane potential used in the test pulse, both theoretically and, within measurement error, experimentally.

A useful ratio for calculating the parameters of the model is that obtained from

threshold charge displacements. The ratio of the threshold charge in the partially inactivated to that in the fully primed states is obtained from eqns. (6) and (11) together with (13) and is given by

$$(Q'_{th}/Q_{th}) = (Q'/Q)\left[\frac{u'_{th}+R(u'_{th})^n}{u_{th}+Ru_{th}^n}\right]. \quad (15)$$

Eliminating u'_{th} from eqn. (15) using eqn. (14) gives

$$(Q'_{th}/Q_{th}) = (Q'/Q)\left[\frac{u_{th}(Q/Q')^{1/n}+Ru_{th}^n(Q/Q')}{u_{th}+Ru_{th}^n}\right]. \quad (16)$$

Since Q'_{th}/Q_{th} and Q'/Q are measured parameters, eqn. (16) contains two unknowns, u_{th} and R.

TABLE 3. Values of parameters for the relation $Q_{th} = K(u_{th}+Ru_{th}^n)$ calculated from values of Q and Q_{th} measured in fully polarized and partially depolarized fibres

Parameter	$n=2$	$n=3$	$n=4$	$n=5$
u_{th}	0·57	0·69	0·76	0·80
u_{th}^n	0·32	0·33	0·33	0·33
R	1·29	2·56	3·31	3·80
K(nC/μF)	11·62	7·48	6·18	5·54

The values are calculated based on eqns. (18) to (21) with $(Q'/Q) = 0{\cdot}60$, $(Q'_{th}/Q_{th}) = 0{\cdot}87$, $Q_{th}/Q_{max} = 0{\cdot}43$ and $Q_{max} = 26{\cdot}6$ nC/μF.

A second equation relating R and u_{th} is that for Q_{th}/Q_{max}. Setting $u = 1$ in eqn. (4) gives Q_{max} which, together with Q_{th} from eqn. (6), gives

$$Q_{th}/Q_{max} = (u_{th}+Ru_{th}^n)/(1+R) \quad (17)$$

or

$$R = \frac{u_{th}-(Q_{th}/Q_{max})}{(Q_{th}/Q_{max})-u_{th}^n}. \quad (18)$$

Eliminating R from eqn. (16) using eqn. (18) one obtains an equation having u_{th} as the sole unknown,

$$A+Bu_{th}^{n-1}+Cu_{th}^n = 0. \quad (19)$$

The values of the parameters A, B and C in eqn. (19) can be determined from experimental measurements for any assumed value of n. They are given by

$$A = (Q_{th}/Q_{max})(Q'_{th}/Q_{th})(Q/Q')-(Q_{th}/Q_{max})(Q/Q')^{1/n}, \quad (20)$$

$$B = (Q/Q')(Q_{th}/Q_{max})-(Q_{th}/Q_{max})(Q'_{th}/Q_{th})(Q/Q') \quad (21)$$

and

$$C = (Q/Q')^{1/n}-(Q/Q'). \quad (22)$$

Values of u_{th}, u_{th}^n and R calculated by eqns. (18) and (19) for n values from 2 to 5 are presented in Table 3. The calculations were carried out using the mean values of 0·60 and 0·87 for Q'/Q and Q'_{th}/Q_{th} (Table 2). Q_{th}/Q_{max} was set equal to 11·5/26·6, where 11·5 nC/μF is mean value of Q_{th} in fully polarized fibres and 26·6 nC/μF is the value of Q_{max} estimated from the mean Q *vs.* V data from fibres with contraction blocked by high internal EGTA (Horowicz & Schneider, 1981). The calculated value

of u_{th} varies from 0·57 to 0·80 as n varies from 2 to 5. Depending on the value of n, about 60–80 % of the charge groups of reaction A must thus be in the initiator position in order to achieve a just-detectable contraction under full polarization. The value of R varies from 1·3 to 3·8 as n increases from 2 to 5. This signifies that the charge movement associated with the second reaction contributes more than half of the measured Q_{max}. The values of K determined for each n from the calculated R together with the value of 26·6 nC/μF for Q_{max} are also presented in Table 3. The value of K falls as R increases with increasing n, since Q_{max} has a constant value.

Although one could determine, in principle, the value of n from the behaviour of Q_{th} in response to gradual inactivation (see eqn. (8)), the results are too scattered to be of practical value in this regard. Other kinds of data are required to determine n.

Critically activated state

It is of interest to consider the special case where the fibres are inactivated to the point where Q_{max} is the rheobase ($Q^*_{th} = Q^*_{max}$). For convenience, this case will be called the critically activated state and will be denoted by starred parameters. For the critically activated state $u = 1$ at threshold: thus the threshold condition given by eqn. (10) becomes

$$Q_{B\,th} = K^*R, \tag{23}$$

and eqns. (11) to (13) become

$$Q^*_{th} = K^*(1+R) = Q^*_{max} \tag{24}$$

and

$$u^n_{th} = (K^*/K) = (Q^*/Q). \tag{25}$$

Eqn. (25) indicates that the value of u^n_{th} can be used to predict the fraction of charge movement which should remain in the critically activated state. Measurements on fully polarized and partially depolarized, but still-contracting fibres gave the u_{th} values in Table 3. The resulting value of u^n_{th} was 0·33, independent of the value used for n. Thus 33 % of charge movement is predicted to remain in the critically activated state. This prediction can be compared with charge measurements in three runs in which fibres were sufficiently depolarized to eliminate contraction. Slight further polarization restored the ability to contract, so these runs were carried out at depolarizations to just beyond the critically activated state. In these runs 30–45 % of charge movement remained, in rough agreement with the value of 33 % predicted for the critically activated state.

The definition of the critically activated state also gives

$$Q^*_{max}/Q_{th} = (Q_{max}/Q_{th})\,(Q^*/Q). \tag{26}$$

In the three runs in the non-contracting state the maximum charge moved was found to be about 77 % of Q_{th} for the fully polarized state. This value agrees well with the prediction of 0·77 for Q^*_{max}/Q_{th} obtained by eqn. (26), using 0·43 for Q_{th}/Q_{max} and 0·33 for Q^*/Q. The observations on fibres sufficiently depolarized to eliminate contraction completely thus appear to be generally consistent with the model.

Steady-state Q vs. *V relation*

Up to this point, no use has been made of the explicit voltage and time dependence of the u variable. In the model, the steady-state Q *vs.* V relation is determined by eqn. (4) and the steady-state u *vs.* V relation. If one assumes that the charged groups in the first reaction distribute between the two available positions in accord with Boltzmann statistics, then as Schneider & Chandler (1973) have shown

$$u = \frac{1}{1+\exp[-(V-\bar{V})/k]}, \tag{27}$$

where $\bar{V}$ is the membrane potential at which the two positions have equal probability of occupancy and k detemines the maximum steepness of the change in the ratio of

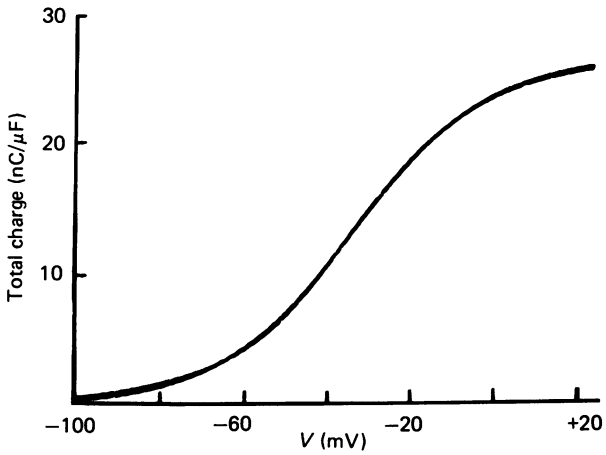

Fig. 18. Steady-state Q *vs.* V relations for different values of n in the equations: $Q = K(u + Ru^n)$ and $u = (1+\exp-[(V-\bar{V})/k])^{-1}$. Five curves are superimposed, corresponding to integer values of n from 1 to 5. The constants used in the calculations were:

	$n=1$	$n=2$	$n=3$	$n=4$	$n=5$
R	0	1·29	2·56	3·31	3·80
K(nC/μF)	26·6	11·8	7·61	6·26	5·60
Q_{max}(nC/μF)	26·6	27·0	27·1	27·0	26·9
$\bar{V}$(mV)	−33·0	−42·3	−52·4	−59·3	−64·3
k(mV)	16·6	18·1	19·0	19·2	19·2

The constants were obtained by fitting the equations to the data given in Fig. 9 of the previous paper (Horowicz & Schneider, 1981). The values for $n = 1$ correspond to those presented for the simple two-state Boltzmann model in that paper. The procedures followed are described in the text.

the occupancy probabilities for an e-fold change in membrane potential. Note that in this and subsequent results sections $\bar{V}$ and k denote parameters describing the steady-state u *vs.* V relation rather than those describing over-all Q *vs.* V.

In fitting any set of Q *vs.* V data with the combination of eqns. (4) and (27), there are five available parameters to adjust. One can fix n and R as a pair using the threshold charge results summarized in Table 3, thus leaving only three adjustable

parameters for the fit – i.e. K, $\bar{V}$ and k. Proceeding along these lines and using the average Q *vs.* V data given in the previous paper (Horowicz & Schneider, 1981) for fibres exposed to 20 mM-EGTA at their cut ends, the fits obtained for values of n from 1 to 5 are shown in Figure 18. Although there are small numerical differences in the calculated values of Q, for all practical purposes the fitted curves virtually superimpose on each other each curve represents quite well the experimental points, which appear in Fig. 9 of the previous paper together with their fit for $n = 1$. Clearly, the steady-state Q *vs.* V data cannot be used to extract the appropriate value for n for the model. For this purpose, another approach has to be taken.

Comparison of experimental and calculated I_Q values

The approach that was most successful in selecting the probable value of n involved fitting the models to the currents produced by the charge movements. The forms of the functions fitted during the test pulses were obtained by differentiating the total charge displacement as given by eqn. (4) with respect to time: i.e.

$$\frac{dQ}{dt} = I_Q = K\frac{du}{dt} + K \cdot R\frac{du^n}{dt} \tag{28}$$

or

$$I_Q = K(1 + nRu^{n-1})\frac{du}{dt}. \tag{29}$$

The time course of the u variable is assumed to be described by the relation

$$u = u_f - (u_f - u_i)\exp -(t/\tau_u). \tag{30}$$

In these equations K and R are the constants appropriate for the chosen value of n; u_i is the initial value of u and u_f the final value for a pulse of sufficient duration to reach a steady-state value of u; and τ_u the settling time constant of the u variable for the specified test pulse. Differentiating u as given by eqn. (30) with respect to time and substituting the result into eqn. (29) one obtains

$$I_Q = (K/\tau_u)[(u_f - u) + nR(u_f u^{n-1} - u^n)]. \tag{31}$$

Eqns. (30) and (31) were used to calculate the theoretical ON time course of I_Q for comparison with the measured ones. Theoretical I_Q OFFs were not calculated because the observed I_Q OFF time courses approached those of the linear fibre capacitance and were thus probably limited by the speed of the clamp. The first aim of the ON time-course analysis was to determine the likely value of n. The results from several fibres were examined by fitting the steady-state Q *vs.* V data obtained from each fibre using eqns. (4) and (27) for various positive integer values of n. For each pair of n and R values (Table 3) the corresponding values of K, $\bar{V}$ and k were determined as described above for Fig. 18. Theoretical currents were calculated using the same K and R values. In addition, specific values for the parameters u_f and u_i were determined from the charge movement measurements. The value of u_f was calculated from eqn. (4) using K, R and the chosen n with $Q = Q_{ON}$, where Q_{ON} was the average total charge measured with a long-duration pulse, usually 100 or 50 msec depending on pulse amplitude. Because of the finite speed of the voltage-clamp and the probable cable delays along the fibre and into the T-system, the calculations of I_Q were started at the fifth interval into the pulse, i.e. after 4 msec. Therefore, u_i for

the fifth interval was calculated from eqn. (4) with the same values of K, R and n used for u, but with

$$Q = \sum_{i=1}^{4} I_Q(i) \cdot \Delta t,$$

where $I_Q(i)$ is the measured current in the ith interval after the start of the pulse and

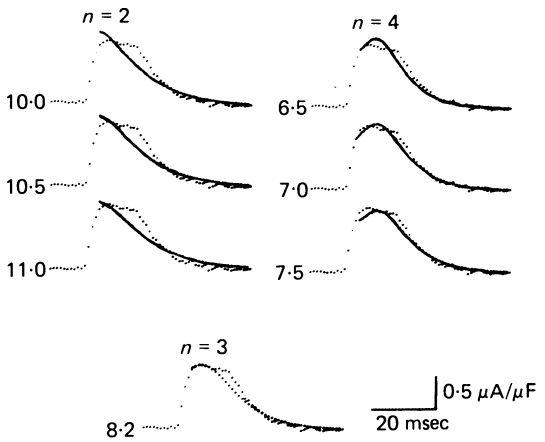

Fig. 19. Comparison of calculated values of I_Q with a measured I_Q record in response to a +70 mV pulse. The same measured record is used in each pair of traces (same fibre as in Fig. 10 of preceding paper, run 1; $V_H = -92$ mV). The first point in each calculated sequence is for the fifth interval after the start of the pulse; the duration of each interval is 1 msec. The three comparisons in the upper left are for $n = 2$ with τ_u chosen to be 10·0, 10·5 and 11·0 msec. In the upper right the comparisons are for $n = 4$ with τ_u chosen to be 6·5, 7·0 and 7·5 msec. The bottom comparison is for $n = 3$ with τ_u equal to 8·2 msec. For clarity the calculated points are connected by a continuous curve for the comparisons when $n = 2$ and $n = 4$.

For each value of n, the calculations were based on the following steps:

(i) R was obtained from Table 3 for the chosen value of n.

(ii) K was obtained by fitting eqns. (4) and (18) to the steady-state Q *vs.* V data obtained for this fibre using the methods outlined in Fig. 18 and the text.

(iii) Using the measured I_Q *vs.* time record being fitted, u_i and u_f were obtained from eqn. (4) where Q is equated with the integral of I_Q during the first 4 msec after the start of the pulse for u_i and $Q = Q_{ON}$ for u_f. R from step (i) and K from step (ii) were used in eqn. (4).

(iv) A value of τ_u was chosen.

(v) I_Q was calculated from eqns. (21) and (22) using the values of the parameters resulting from steps (i) to (iv).

Δt is the interval duration, which was 1 msec. For all subsequent times eqns. (30) and (31) were used in the calculations of I_Q, with τ_u being the only adjustable parameter.

Fig. 19 illustrates the comparisons between several calculations and the measured I_Q in response to a pulse to −22 mV. In each of the seven pairs of curves the same experimental record is reproduced. The measured I_Q rises to an early peak, subsides to a plateau and finally declines rapidly to the base line. The three pairs of curves in the upper left give the comparisons with calculations for $n = 2$; the calculated

curves start at the fifth interval after the start of the pulse. The upper comparison is for $\tau_u = 10{\cdot}0$ msec, the middle for $\tau_u = 10{\cdot}5$ msec and the lower for $\tau_u = 11{\cdot}0$ msec. It is apparent that all the calculated curves decline monotonically without any sign of a maximum and without any appreciable segment of adjacent points in the

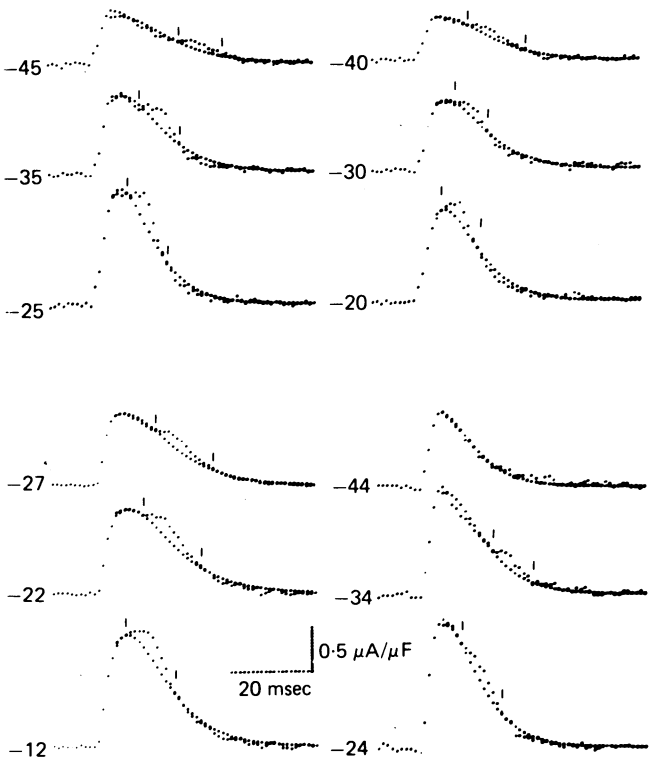

Fig. 20. Comparison of calculated I_Q values taking $n = 3$ with measured I_Q records in response to depolarizing pulses obtained from four fibres. Each pair of traces is composed of a measured I_Q record and a calculated sequence; the calculated sequence begins with the fifth interval after the start of the pulse. The details of the calculations are given in Fig. 19 and the text. The placement of vertical bars is described in the text. Each quadrant shows comparisons for three pulse amplitudes obtained in an individual fibre. The internal potential (mV) is given for each pair of traces. The fibre references and best-fit τ_u values are as follows. Upper-left quadrant: fibre 116, run 1; $V_H = -105$ mV; $\tau_u = 8{\cdot}5$, $7{\cdot}25$ and $6{\cdot}0$ msec for -45, -35 and -25 mV respectively. Upper-right quadrant: fibre 75, run 3; $V_H = -100$ mV; $\tau_u = 7{\cdot}9$, $7{\cdot}0$ and $6{\cdot}2$ msec for -40, -30 and -20 mV respectively. Lower-left quadrant: fibre 76, runs 1 and 2; $V_H = -92$ mV; $\tau_u = 8{\cdot}25$, $8{\cdot}2$ and $7{\cdot}3$ msec for -27, -22 and -12 mV respectively. Lower-right quadrant: fibre 84, run 1 ($l_C = 634$ μm, $s = 2{\cdot}56$ μm, $d = 74$ μm; temperature 2 °C); $V_H = -104$ mV; $\tau_u = 5{\cdot}7$, $6{\cdot}4$ and $5{\cdot}75$ msec for -44, -34 and -24 mV respectively. Data for fibres 116, 75 and 76 appear in legends to Figs. 11, 1 and 10 of the preceding paper.

experimental curve being adequately reprodued. A further lengthening of τ_u would only lower the early points and raise the later ones. The three pairs of curves in the upper right of Fig. 19 give the comparisons with calculations for $n = 4$. The upper comparison is for $\tau_u = 6{\cdot}5$ msec, the middle for $\tau_u = 7{\cdot}0$ msec and the lower for

τ_u = 7·5 msec. In each of the calculated curves the current increases to a single maximum and thereafter declines monotonically to zero. The calculated maxima come later than the measured maximum current and earlier than the later portion of the plateau. In the upper two comparisons the calculated maximum overshoots the measured current while in the lower it just matches the early part of the plateau at the cost of lowering points on either side of the maximum below the measured values. Again, no sequence of adjacent intervals in the experimental record is well

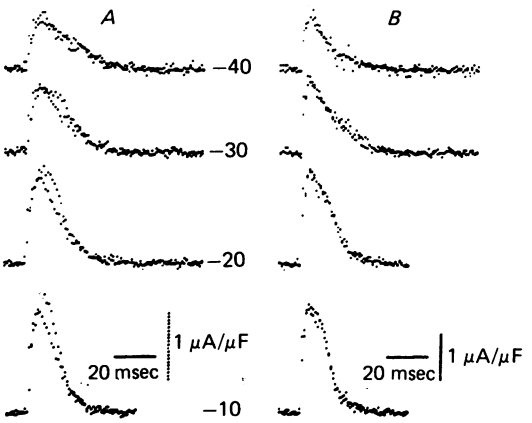

Fig. 21. Comparison of I_Q time courses for the same pulses under full polarization and steady partial depolarization. Records obtained under partial depolarization were scaled up as described in the text. Numbers between pairs of traces give V'_m (mV) during the pulse. *A*, fibre 113, average of runs 5 and 8 (V_H = −100 mV) and average of runs 6 and 7 (V_H = −55 mV); l_C = 836 μm, s = 2·18 μm, d = 77 μm. *B*, fibre 91, average of runs 1 and 4 (V_H = −100 mV) and run 3 (V_H = −60 mV); l_C = 608 μm, s = 2·54 μm, d = 58 μm. Temperature 1·5–2·3 °C.

reproduced within the level of noise. The pair of curves at the bottom of Fig. 19 gives the comparison of the calculated curve for n = 3 and τ_u = 8·2 msec. In this case, the experimental maximum and its adjacent intervals are well fitted, but not the plateau. The later portion of the plateau could not be reproduced for any value of n that was reasonably small. In some fibres, for example where the charge movement currents have a second maximum rather than a plateau, values of n up to 6 could not produce anything like adequate fits to the second maximum. Many calculations were made in the manner described using measurements from several fibres, and for each fibre the best fit to the early maximum was obtained with n = 3.

Fig. 20 illustrates experimental records and the fits obtained with n = 3 in four different fibres each for three depolarizing pulses. The results from each fibre are displayed in one quadrant. A small extra current, which is not reproduced by the calculations, appears to be present during the latter part of almost all experimental records over the intervals marked by vertical bars. This extra current appears to increase in size and to occur earlier in the declining phase of the transient as the pulse amplitude is increased. For the largest pulse in Fig. 20 it appears to begin near the

time of the early maximum. Taking the difference between observed and calculated records over the intervals marked by vertical bars in Fig. 20 to constitute the non-reproduced current, it was found to contribute from 0·5 to 1·6 nC/μF of charge to the various records. Its relative contribution ranged from 3·8 to 7·4 % of Q_{ON}. The observed current which is not described by the model thus appears to be a minor but not negligible component of the overall charge movement. One possible explanation for this extra current is that it may be a result of the calcium release process from the terminal cisternae. As circumstantial evidence one might note that the extra current begins at times which coincide with or slightly precede the contraction threshold durations when the cut end of the fibre is exposed to 1 mM-EGTA.

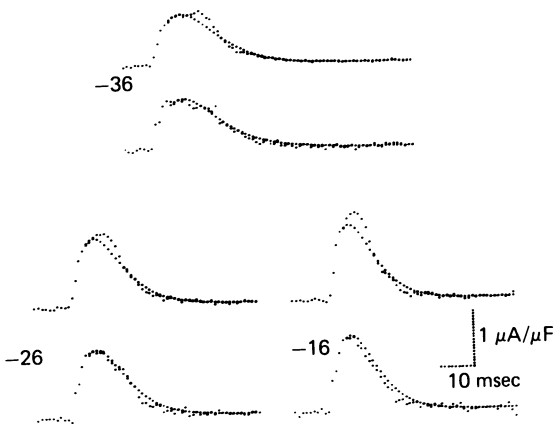

Fig. 22. Comparisons of calculated I_Q records with I_Q records measured for the same pulses under full polarization and under steady partial depolarization. Each of the three panels is composed of two pairs of records. The upper pair gives I_Q measured under full polarization and the I_Q record calculated so as to approximate it most closely. The lower pair gives the same calculated I_Q record and I_Q measured under partial depolarization and scaled as described in the text. The number in each panel gives V'_m (mV) during the pulse τ_u = 8·3 msec for upper panel, 6·7 msec for lower left and 5·8 msec for lower right. Same fibre as in Fig. 9, runs 5 and 8 (V_H = −96 mV) and run 6 (V_H = −66 mV).

Effect of steady partial depolarization on charge movement kinetics

If the extra charge movement current which is not accounted for by the model is a result of calcium release from the sarcoplasmic reticulum, steady partial fibre depolarization might be expected to decrease it relatively more than the overall charge. To investigate this possibility I_Q records from runs under partial depolarization were compared with the average of I_Q records from bracketing control runs for the same pulse under full polarization. Fig. 21 presents pairs of such records for four different pulses in two different fibres, results from each fibre being displayed in one column. Each record under partial depolarization was scaled up so that its area from pulse ON to 2 msec before t_{th} for full polarization equalled the area over the same interval under full polarization. This scaling procedure should have been minimally influenced by the extra current, which only began at or slightly before t_{th}. For the three lower pairs of records of Fig. 21*A* the intermediate portion of each

scaled-up record under partial depolarization passed below its paired record obtained under full polarization. In fact, the record pairs in Fig. 21 *A* resemble those in Fig. 20, indicating that for this fibre steady partial depolarization seemed to suppress the current not accounted for by the model relatively more than the overall charge.

Pairs of records similar to those shown in Fig. 21 *A* were observed in about half the cases. In the other fibres, exemplified by Fig. 21 *B*, the same scaling procedure as used in *A* produced pairs of records which matched closely over their entire time courses. According to the preceding reasoning, such fibres should have had little or no charge movement which could not be accounted for by the model, even under full polarization. Analysis of records from such fibres showed this to be the case.

Fig. 22 presents an analysis of I_Q kinetics from another fibre in which the scaled-up I_Q under partial depolarization passed below the shoulders or bumps in paired records under full polarization. The upper pair of records in each panel shows I_Q under full polarization and the calculated model record which most closely approximated it. As usual, the calculated records also passed below the observed shoulders or bumps. The lower pair of records in each panel shows the same calculated record compared with the I_Q observed under partial depolarization scaled up using the same procedure as in Fig. 21. These observed records follow the calculated ones quite closely, tending to confirm the hypothesis that the extra component not accounted for by the model is relatively less pronounced under steady partial depolarization.

Voltage dependence of u transition time constant and potential energy barrier location

The time course of the currents associated with charge movements are manifestly membrane-potential-dependent. If the model has validity then one might expect that the τ_u values giving the best fits for different potentials should vary in a systematic way with V. In particular, the model should provide the relation between τ_u and V. If the standby and initiator positions of the first reaction are separated by a single potential barrier then the rate constant for particles moving from the standby to the initiator position, $\alpha_u(V)$, is given by

$$\alpha_u(V) = \alpha_u(\overline{V})\exp[\eta(V-\overline{V})/k], \tag{32}$$

while the rate constant for particles moving in the reverse direction, $\beta_u(V)$, is given by

$$\beta_u(V) = \alpha_u(V)\exp-[(V-\overline{V})/k]. \tag{33}$$

In these relations, $\alpha_u(\overline{V})$ is a constant having the value of $\alpha_u(V)$ when $V = \overline{V}$, η is the distance from the barrier peak to the standby position expressed as a fraction of the total distance between the two positions, and $\overline{V}$ and k have their usual significance, but apply here only to the first reaction. Details can be found in the review by Adrian (1978), which gives a clear exposition of the assumptions and basic relations for a single barrier model. For a step pulse in potential the particles approach an equilibrium distribution with an exponential time course having a time constant, $\tau_u(V)$, given by

$$\tau_u(V) = 1/[\alpha_u(V)+\beta_u(V)]. \tag{34}$$

Introducing eqns. (32) and (33) into this relation yields

$$\tau_u(V) = 2\tau_u(\overline{V})/\exp[\eta(V-\overline{V})/k]\cdot\{1+\exp-[(V-\overline{V})/k]\}. \tag{35}$$

where $\tau_u(\bar{V})$ is a constant which has the value of $\tau_u(V)$ when $V = \bar{V}$ and is also given by the relation

$$\tau_u(\bar{V}) = 1/2\alpha_u(\bar{V}). \tag{36}$$

In order to extract the values of $\tau_u(\bar{V})$ and η in any one experiment it is useful to rearrange eqn. (35) to give

$$1/\tau_u(V)\{1+\exp-[(V-\bar{V})/k]\} = (1/2\tau_u(\bar{V}))\cdot\exp[\eta(V-\bar{V})/k]. \tag{37}$$

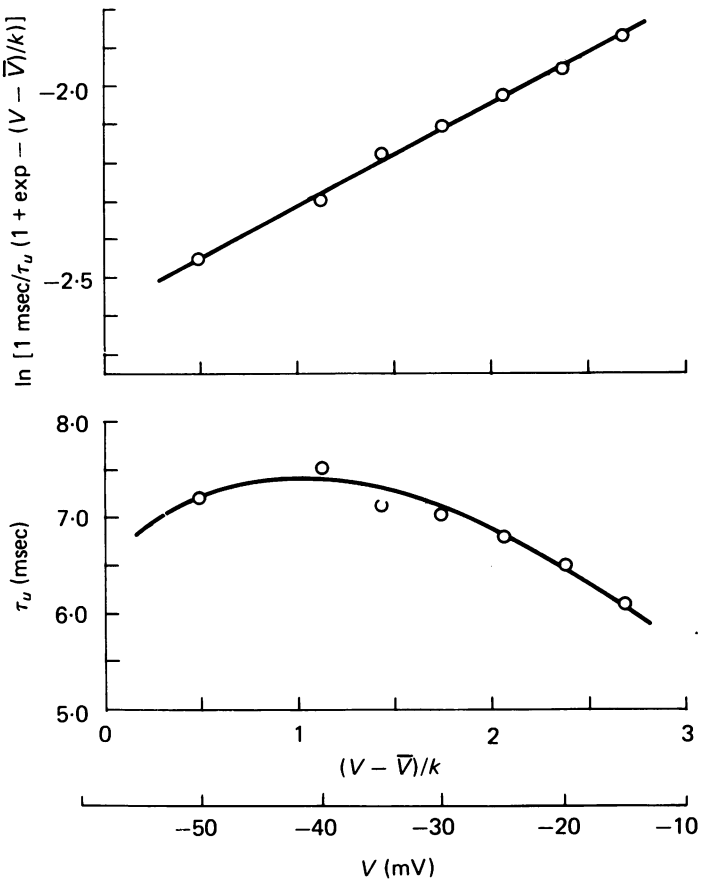

Fig. 23. The relation between the best-fit τ_u ($n = 3$) and $(V-\bar{V})/k$ or V. Estimates of $\bar{V}$ and k were obtained by fitting eqns. (4) and (18) to the steady-state Q *vs.* V for the fibre as outlined in Fig. 18, assuming $n = 3$. The best fit τ_u values were determined by each pulse as outlined in Fig. 19 and the text. The ordinate in the upper graph gives the values of $\ln[1\ \text{msec}/\tau_u(1+\exp-(V-\bar{V})/k)]$. The continuous line is a least-squares fit of eqn. (29) to the points. The ordinate in the lower graph gives the values of the best-fit τ_u values. In this graph the curve is a plot of eqn. (26) using the value of $\tau_u(\bar{V})$ and n determined from the upper graph. $\bar{V} = 57{\cdot}8$ mV, $k = 16{\cdot}0$ mV. Same fibre as in Fig. 3.

Taking the natural logarithm of the last expression, one obtains

$$\ln(\tau_u(V)^{-1}/\{1+\exp-[(V-\bar{V})/k]\}) = \ln(1/2\tau_u(\bar{V})) + \eta(V-\bar{V})/k, \tag{38}$$

which indicates that the expression on the left-hand side is linearly related to $(V-\bar{V})/k$ where η is the slope and, with an axis chosen at $(V-\bar{V})/k = 0$, $\ln(1/2\tau_u(\bar{V}))$ is the intercept.

Fig. 23 illustrates the use of eqn. (38) in an experiment where the τ_u values which best fit the measured I_Q transients were determined for various potentials as described earlier and illustrated in Fig. 20. The straight line in the upper graph is a fit of eqn. (38) to the experimental data using the least squares method. In the lower graph the points depict the best fit τ_u values as a function of $(V-\bar{V})/k$ and the curve

TABLE 4. Best-fit parameters for voltage dependence of τ_u based on $n = 3$ in eqn. (4).

(1) Fibre reference	(2) $\bar{V}$ (mV)	(3) k (mV)	(4) $\ln[1\ \text{msec}/2\tau_u(\bar{V})]$ estimate ± S.E.	(5) η estimate ± S.E.
38	−50·9	17·1	−2·455 ± 0·033	0·389 ± 0·026
75	−51·2	15·5	−2·803 ± 0·034	0·438 ± 0·027
76	−50·6	17·0	−2·811 ± 0·026	0·375 ± 0·021
82	−57·8	16·0	−2·576 ± 0·015	0·263 ± 0·008
84	−48·3	18·7	−2·513 ± 0·045	0·356 ± 0·029
116	−50·3	11·5	−2·792 ± 0·041	0·357 ± 0·022
Mean	−51·5	16·0	−2·658	0·363
S.D. of mean	3·2	2·4	0·162	0·057
S.E. of mean	1·3	1·0	0·066	0·023

is calculated from eqn. (35) using the parameters obtained from the slope and intercept of the straight line in the upper graph. The relations seem to correspond reasonably well with the data. For this experiment $\eta = 0{\cdot}26$ and $\tau_u(\bar{V}) = 6{\cdot}57$ msec. Since $\eta \neq 0{\cdot}5$, the maximum for $\tau_u(V)$ is not at $V = \bar{V}$ and the curve is not symmetrical about the maximum. The value of η obtained in the illustrated experiment is the lowest found in the fibres analysed. Table 4 summarizes the results from six fibres using the analysis outlined. The average value of −2·658 for $\ln[1\ \text{msec}/2\tau_u(\bar{V})]$ corresponds to $\tau_u(\bar{V}) = 7{\cdot}13$ msec. In turn, this means that $\alpha_u(\bar{V}) = 0{\cdot}0701\ \text{msec}^{-1}$. The average value of 0·363 for η implies that the peak of the potential energy barrier is about one third of the way from the standby to the initiator position.

DISCUSSION

The principal new finding reported in this paper is that the charge Q_{th} moved during pulse durations which produced microscopically just-detectable contraction had the same value for pulses to different membrane potentials. Q_{th} also had the same value for a given pulse applied either alone or together with an immediately preceding prepulse to below rheobase for contraction. These observations demonstrate a clear correlation between charge movement and one index of contractile activation. They establish at least a parallelism between charge movement and one or more steps in the depolarization–contraction coupling process. They also appear to be consistent with charge movement's serving as the voltage-sensitive step in depolarization–contraction coupling.

In the process of studying Q_{th} several observations were also made concerning the time course of charge movement currents. The non-exponential nature of I_Q for pulses to between roughly -50 and -20 mC (Almers, 1975; Almers *et al.* 1975; Adrian & Peres, 1977) was quite pronounced in the present studies on fibres with maintained contractile activity. Prolonged tails, shoulders, secondary rising phases and early flat segments were routinely observed in I_Q records for depolarizations to potentials increasingly beyond rheobase for contraction. Such complex time courses indicate the existence of multiple Q components. It was also observed that prepulses to potentials below rheobase for contraction did not seem to alter the latter part of I_Q for an immediately following contraction-inducing test pulse. Such prepulses apparently only eliminated the initial segment of the I_Q record for the test pulse alone and advanced the latter segment to earlier in time. This observation indicates that the mix of Q components moved by the prepulse may have been the same as the mix moved during the initial period of the test pulse. In general terms, the charge components that moved first as a function of increasing depolarization thus appeared to be those that also moved first in time during a single relatively large depolarization.

The model introduced to interpret the present results is one which might be expected to reproduce the I_Q kinetic properties outlined in the preceding paragraph. In the model there are two Q components. Component A follows first-order kinetics and is produced by movement of charges between two intramembrane sites separated by a single energy barrier. Component B is instantaneously proportional to an integer power n of the fraction of component A charges which have moved across the energy barrier from the site they occupy when the membrane potential is highly negative. Since the amount Q_B of B which is observed is an instantaneous function of the amount Q_A of A which has moved, the sequence of mixes of A and B occurring with increasing depolarization must be the same as the sequence occurring with time during a single depolarization. Steady partial depolarization is assumed to scale down components A and B by the same factor.

The model accounts for our observations regarding Q_{th} if it is further assumed that the pulse duration required to produce just-detectable contraction corresponds to the time required to move the same set amount $Q_{B\,th}$ of component B charge under both full polarization and steady partial depolarization. The fact that the overall Q_{th} is constant in fully polarized fibres will automatically ensure that $Q_{B\,th}$ is also constant, since under full polarization the mix of Q_A and Q_B in a given overall Q is always the same. On the other hand, steady partial depolarization increases the proportion of Q_B in a given overall Q compared with the proportion of Q_B in the same Q under full polarization. The condition that $Q_{B\,th}$ be constant thus necessitates that the value of the overall Q_{th} decrease during steady partial depolarization, as we have observed. The measured fractional depressions of Q and Q_{th} produced by steady partial depolarization can in fact be used to calculate the fractions $1/(1+R)$ and $R/(1+R)$ of the overall Q_{max} contributed respectively by components A and B for any assumed value of the power n. They can also be used to calculate the fraction of the total available amount of each component which must be moved to attain Q_{th} under either full polarization or steady partial depolarization, again for any value of n.

Using the R values obtained from the average depression of Q and Q_{th} under steady partial depolarization, the I_Q records presented here were best fitted using $n = 3$, with

which both the relatively early and late portions of most I_Q records could be reproduced. Theoretical records calculated for other values of n did not succeed in reproducing as many sequential points of the I_Q records as could be reproduced using $n = 3$.

The best fits of the $n = 3$ model did not, however, succeed in reproducing the entire time course of many I_Q records. They systematically passed below the shoulders, secondary rising phases and later portions of early flat segments of I_Q records during depolarizations to the voltage range somewhat beyond rheobase for contraction. Such non-reproduced elements may have been due to a relatively small amount of charge movement contributed by one or more processes which were not included in the present model. It is interesting to note in this regard that concentrations of tetracaine which block contraction also appear to eliminate the secondary rising phases in I_Q records (R. H. Adrian & C. Caputo, personal communication) and that steady partial depolarizations which depress contractile activity also decrease the non-reproduced current relatively more than the overall charge movement. The start of such non-reproduced elements also either coincided with or began slightly before the pulse duration required to produce just-detectable contraction. Therefore, an attractive possibility is that the non-reproduced currents were somehow associated with calcium release from the sarcoplasmic reticulum (SR). This might have been the case if calcium release were accompanied by a slight extra depolarization of the T-tubule membrane. Two mechanisms, which to our knowledge were first suggested by Dr W. K. Chandler, could produce such an effect. First, a voltage drop may be present owing to calcium ions moving along an electrically resistive pathway extending from the T/SR interspace to the bulk of the myoplasm. Alternatively, a change in the T-tubule surface potential could be produced by elevated calcium in the T/SR interspace resulting from release of calcium by the adjacent terminal cisternae. Although the extra current was not much modified by exposure of the cut ends to 20 mM-EGTA, the calcium concentration in the T/SR interspace might still have increased to high concentrations rapidly so as locally to saturate the EGTA present even at a concentration of 20 mM. Another possibility is that the reaction with EGTA could be slow enough so as not to bind appreciable calcium in the interspace during the rapid phase of release but be fast enough to compete with the tropinin sites as the calcium diffuses out of the interspace into the region occupied by the filaments.

If the extra current not accounted for by the model were due to a small depolarizing change in the T-tubule membrane potential, the magnitude of such a potential change could be determined from the charge carried by the extra current and the Q *vs.* V relationship. Using the average of the extra currents from the records in Fig. 20 and the average Q *vs.* V relationship presented in Fig. 9 of the preceding paper (Horowicz & Schneider, 1981), the potential change was calculated to be 2·5 mV at about −40 mV, 2·2 mV at about −30 mV and 3·5 mV at about −20 mV. Since τ_u decreases with increasing depolarization over this range of potentials (Fig. 23), the tendency of the final tails of the calculated records to decay slightly more slowly than the observed records (Fig. 20) may have been caused by not considering the slight decrease in τ_u which would be produced by the slight extra depolarization.

Adrian & Peres (1977) have already put forward a specific example of the type of kinetic scheme used here. They proposed that I_Q equal the sum of two terms, one

proportional to the rate of change of the Hodgkin–Huxley (1952) variable for activation of delayed rectification in skeletal muscle (Adrian *et al.* 1970) and the second proportional to the rate of change of the fourth power of that variable. Adrian & Peres (1977) also suggested that their kinetic scheme, which is equivalent to the present model with $n = 4$, could account for the bumps and secondary rising phases in various I_Q records. We have tested this suggestion with the present model and have found that if the model parameters are restricted so as to agree with both the observed average depression of Q and Q_{th} under steady partial depolarization and the Q *vs.* V results from a particular fibre, the secondary rising phases in the I_Q records from that fibre could not be reproduced using any n value from 2 to 6.

The values of threshold charge movement measured for cut fibres in this study are somewhat higher than those found on intact fibres. Almers & Best (1976) obtained 8·66 nC/μF for Q_{th} in fully primed intact fibres, which is 75 % of the 11·5 nC/μF value found here on cut fibres. In terms of the model presented here, experiments designed to measure threshold charge when contraction reappears during the process of repriming provide estimates of Q_{th} for the critically activated state. In such experiments Adrian, Chandler & Rakowski (1976) obtained a value of about 3·5 nC/μF for Q^*_{th} on intact fibres. This is 40 % of the Q^*_{th} value of 8·8 nC/μF found here for critically activated cut fibres using the estimate of 0·76 for Q^*_{th}/Q_{th} with $Q_{th} = 11{\cdot}5$ nC/μF. The reason for these discrepancies is most likely to be found in the different solutions used on cut fibres compared with intact fibres, and perhaps in the possibility of participation of membrane calcium currents (Horowicz & Schneider, 1981) in the long post-pulses to about +40 mV used by Adrian *et al.* (1976).

REFERENCES

Adrian, R. H. (1978). Charge movement in the membrane of striated muscle. *A. Rev. Biophys. Bioeng.* **7**, 85–112.

Adrian, R. H. & Almers, W. (1976). Charge movement in the membrane of striated muscle. *J. Physiol.* **254**, 339–360.

Adrian, R. H., Chandler, W. K. & Hodgkin, A. L. (1970). Voltage clamp experiments in striated muscle fibres. *J. Physiol.* **208**, 607–644.

Adrian, R. H., Chandler, W. K. & Rakowski, R. F. (1976). Charge movement and mechanical repriming in striated muscle. *J. Physiol.* **254**, 361–388.

Adrian, R. H. & Peres, A. R. (1977). A gating signal for the potassium channel? *Nature, Lond.* **267**, 800–804.

Adrian, R. H. & Peres, A. (1979). Charge movement and membrane capacity in frog muscle. *J. Physiol.* **289**, 83–97.

Almers, W. (1975). Observations on intramembrane charge movements in skeletal muscle. *Phil. Trans. R. Soc.* B **270**, 507–513.

Almers, W., Adrian, R. H. & Levinson, S. R. (1975). Some dielectric properties of muscle membrane and their possible importance for excitation–contraction coupling. *Ann. N.Y. Acad. Sci.* **264**, 278–292.

Almers, W. & Best, P. M. (1976). Effects on tetracaine on displacement currents and contraction of frog skeletal muscle. *J. Physiol.* **262**, 583–611.

Chandler, W. K., Rakowski, R. F. & Schneider, M. F. (1976). Effects of glycerol treatment and maintained depolarization on charge movement in skeletal muscle. *J. Physiol.* **254**, 285–316.

Hodgkin, A. L. & Horowicz, P. (1960). Potassium contractures in single muscle fibres. *J. Physiol.* **153**, 386–403.

Hodgkin, A. L. & Huxley, A. F. (1952). A quantitative description of membrane current and its application to conduction and excitation in nerve. *J. Physiol.* **117**, 500–544.

HOROWICZ, P. & SCHNEIDER, M. F. (1981). Membrane charge movement in contracting and non-contracting skeletal muscle fibres. *J. Physiol.* **314**, 565–593.

KOVÁCS, L., RÍOS, E. & SCHNEIDER, M. F. (1979). Calcium transients and intramembrane charge movement in skeletal muscle fibres. *Nature, Lond.* **279**, 391–396.

RAKOWSKI, R. F. (1978). Reprimed charge movement in skeletal muscle fibres. *J. Physiol.* **281**, 339–358.

SCHNEIDER, M. F. & CHANDLER, W. K. (1973). Voltage dependent charge movement in skeletal muscle: a possible step in excitation–contraction coupling. *Nature, Lond.* **242**, 244–246.

SCHNEIDER, M. F. & HOROWICZ, P. (1977). Intramembrane charge movement and muscle contraction. *Proc. Int. Union Physiol. Sci.* **13**, 672.

SCHNEIDER, M. F. & HOROWICZ, P. (1978). Intramembrane charge movement and muscle contraction. In *Abstracts of Papers, 144th National Meeting of AAAS* (AAAS Pub. 78-2), p. 41.

SCHNEIDER, M. F. & HOROWICZ, P. (1979). Membrane charge movement at contraction thresholds in skeletal muscle. *Biophys. J.* **25**, 201*a*.